Journal of Iberian Geology (2024) 50:193–223
https://doi.org/10.1007/s41513-024-00229-x

RESEARCH PAPER

Identification and characterisation of seismites in the continental Jurassic red beds: implications for synsedimentary tectonics in the central High Atlas (Morocco)

Ahmed Oussou[1] · Driss Ouarhache[1] · Khadija Boumir[1] · Mustapha Ouaskou[1] · André Charrière[2]

Received: 24 January 2023 / Revised: 7 December 2023 / Accepted: 11 January 2024 / Published online: 14 February 2024

Abstract
The Bathonian-? Late Jurassic red beds outcrop in several synclines in the Moroccan central High Atlas (Imilchil area). They consist in a thick fluvio-lacustrine succession interpreted as the distal part of a large distributive fluvial system. This unit, the Isli Formation, contains different types soft-sediment deformation structures: neptunian dykes, plastic intrusions, load structures, convolute lamination, slumps, water-escape structures (injection dyke and cusps), loop bedding and gravifossum. The deformation mechanisms of these soft-sediment structures are liquefaction and fluidisation of the water-saturated sediments. The tectonic control of sedimentation is evidenced by synsedimentary faults and progressive unconformities at the limbs of the synclines of the region. This indicates that the Isli Formation was deposited in an extensional setting with magmatic activity and salt tectonics. This study reveals that soft-sediment deformation structures were triggered by seismic events, related to the activity of Atlasic faults.

Keywords Soft-sediment deformation structures · Seismites · Distributive fluvial system · Jurassic · High Atlas · Morocco

Resumen
Las capas rojas del Jurásico Superior (Bathoniense?) afloran en varios sinclinales en la zona central del Alto Atlas marroquí (zona de Imilchil). Estos definen una potente sucesión fluvio-lacustre interpretada como la parte distal de un gran sistema fluvial distributivo. Esta unidad, la Formación Isli, presenta diferentes tipos de estructuras de deformación de sedimentos blandos: diques neptúnicos, intrusiones plásticas, estructuras de carga, laminaciones convolutas, slumps, estructuras de escape de agua (diques de inyección y cúspides), loop-bedding y gravifossum. Los mecanismos de deformación de estas estructuras son la licuefacción y fluidización de sedimentos saturados de agua. El control tectónico de la sedimentación se evidencia por fallas sinsedimentarias y discordancias progresivas en los extremos de los sinclinales de la región. Esto indica que la Formación Isli se depositó en un entorno extensional con actividad magmática y tectónica salina. Este estudio revela que las estructuras de deformación de sedimentos blandos fueron provocadas por eventos sísmicos, relacionados con la actividad de fallas atlásicas.

Palabras Clave Estructuras de deformación en sedimento blando · Sismita · Sistema fluvial distributive · Jurásico · Alto Atlas · Marruecos

1 Introduction

Soft-sediment deformation structures (SSDS) are features formed in sediments that are still water-saturated before their consolidation due to liquefaction and fluidisation phenomena (Allen, 1982; Obermieir et al., 2002; van Loon, 2009). There are multiple triggers for these phenomena (Owen, 1987; Owen & Moretti, 2011), but the best-known and most often discussed trigger are earthquakes. Sedimentary beds containing

✉ Ahmed Oussou
ahmed.oussou@usmba.ac.ma

[1] GERA Laboratory, Faculty of Sciences Dhar EL Mahraz, Sidi Mohamed Ben Abdellah University, Fez, BP: 1796, Atlas, 30000 Fez, Morocco

[2] Université Toulouse III -, 13, Terrasses de la Figuière, 30140 Anduze, France

SSDS induced by seismic shaking are called seismites (sensu Seilacher, 1969). In recent decades, this field of study has made considerable progress. Indeed, many special issues on SSDS have been devoted to this field of research, including several papers on seismites (Jones & Preston, 1987; Maltman, 1994; Shiki et al., 2000; Ettonsohn et al., 2002; Van Rensbergen et al., 2003; Storti & Vannucchi, 2007; Owen et al., 2011a; Festa et al., 2014; van Loon, 2014a; Alfaro et al., 2016).

The recognition of seismite beds, such as turbidites and tempestites, requires the verification and validation of several criteria (see Sims, 1975; Wheeler, 2002; Montenat et al., 2007; Owen & Moretti, 2011; Moretti & van Loon, 2014; van Loon, 2014b). Numerous experimental studies using a shaking table have been conducted to investigate and validate certain types of SSDS observed in nature (Dasgupta, 2008; Harris et al., 2000; Kuenen, 1958; Moretti et al., 1999; Nichols, 1995). Some authors have discussed the magnitudes of earthquakes causing the formation of some SSDS types based on their amplitude and the nature of the deformation process (Bachmann & Aref, 2005; Berger & Herwegh, 2019; Berra & Felletti, 2011; Calvo et al., 1998; Ezquerro et al., 2015; Galli, 2000; Guiraud & Plaziat, 1993; Smith & Jacobi, 2002 and references hereafter).

In continental basins, fluvio-lacustrine deposits, mainly in distal fluvial areas and lacustrine facies, are the sediments most susceptible to liquidisation, thus forming soft-sediment deformation structures (Obermeier, 1996; Owen & Moretti, 2011). This is due to the fine grainsize of almost all facies in these depositional environments and their coverage of a wide area.

In Morocco, only a few studies on seismites have been carried out so far. These studies only concern the Pliocene and Quaternary deposits of the Sais Basin (Plaziat & Ahmamou, 1998; Plaziat et al., 2006), the Middle Atlas (Azennoud et al., 2022; Benabbou et al., 2018) and the Moulouya (Zarki et al., 2004).

The aim of this work is to use the fluvio-lacustrine basins of Morocco as a test to examine criteria to recognize seismites. The great variability of SSDS allow examination of their origin. In order to achieve this aim, we carried out a sedimentological and palaeoenvironmental study, a description/classification of the SSDS, and their interpretation in terms of driving forces and deformation mechanisms. Furthermore, this study discusses possible triggers of these SSDS.

2 Geological setting

The Imilchil region is located in the heart of the Central High Atlas (Fig. 1a, b). This part of the Atlas system extends from the central Atlantic to the eastern Mediterranean. It is a typical intracontinental belt, essentially formed by the inversion of Triassic-Liassic rift basins during the convergence of the African and Iberian-European Plate, starting in the Late Cretaceous (e.g., Fekkak et al., 2018; Frizon de Lamotte et al., 2008; Ibouh & Chafiki, 2017; Mattauer et al., 1977). The Central High Atlas is structured in a succession of narrow anticlinal ridges bordering synclinal depressions. The ridges, mostly N70-trending, are aligned with Variscan-aged faults (Escosa et al., 2021; Laville & Piqué, 1992). The cores of these ridges are formed by Triassic evaporitic deposits and the Central Atlantic Magmatic Province (CAMP) basalts (Marzoli et al., 1999, 2019; Panfili et al., 2019), as well as Liassic limestone blocks and Jurassic–Cretaceous magmatic intrusions (Armando, 1999; Barbero et al., 2007; Calvín et al., 2017; Essaifi & Zayane, 2018; Ibouh, 1995, 2004; Ouabid et al., 2021; Zayane et al., 2002). This Jurassic-Cretaceous magmatic activity is interpreted as the result of crustal thinning and the rise of an asthenospheric plume (Frizon de Lamotte et al., 2009). The flanks of the ridges are formed by carbonates ranging in age from Early to Middle Jurassic.

The Jurassic sedimentary series in the axis of the Atlas Belt is organised in a megasequence of about 6000 m thickness, originally divided into an exclusively marine formation (Agoudim Fm) and a regressive detrital formation (Anemzi Fm, Studer, 1987).

In the Imilchil region, this megasequence (Charrière et al., 2011; Ibouh, 1995, 2004) was subdivided into three marine formations (the Tassent Formation, the Bab n'Ouyad Formation and the Tislit Formation), a mixed formation (the Imilchil Formation) and an exclusively continental formation (the Isli Formation). The megasequence ends with the continental Isli Formation (lower Bathonian-? Late Jurassic), which is preserved in the centres of the synclines in the region. This last formation consists of more than 1000 m of fluvio-lacustrine sediments that are very rich in vertebrate footprints, mainly of dinosaurs. A red laguno-continental formation, associated with basaltic flows, unconformably overlies some of the ridges of the folds (Fig. 1b, c). Charrière et al (2009) described the Tasraft Formation which they dated to the Thanetian-? Ypresian based on charophytes and ostracods.

During the deposition of the Jurassic megasequence, the ridges began to grow through the phenomenon of diapirism related to extensional tectonics (Ettaki et al., 2007; Michard et al., 2011; Malaval et al., 2014; Saura et al., 2014; Joussiaume, 2016; Moragas et al., 2018; Martin-Martin et al., 2017; Moragas, 2017; Teixell et al., 2017; Vergés et al., 2017; Dooley & Hudec, 2020; Granado et al., 2021). Diapirism is evidenced by progressive unconformities, synsedimentary normal faults and slumps on the flanks of these ridges and the presence of evaporites in Triassic deposits at the cores of certain ridges (Michard et al., 2011) and in the subsurface (Ayarza et al., 2005) (Fig. 2).

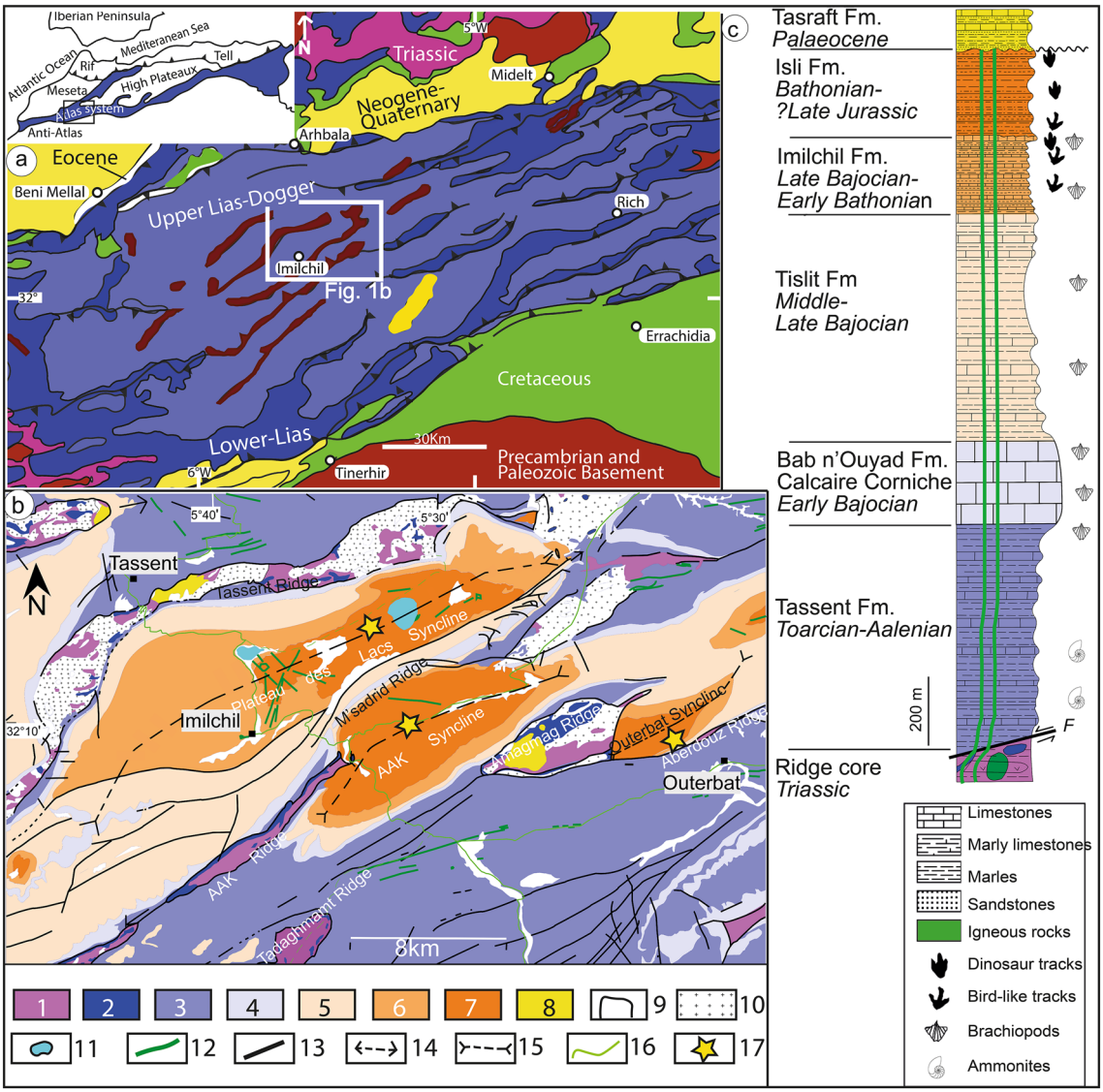

Fig. 1 Geological setting of the studied area. **a** Location of the Central High Atlas in the context of North Africa and its main terrains (modified after the geological map of Morocco at 1,000,000 and Teixell et al., 2003). **b** Geological map of the Imilchil region (modified after the geological maps of Imilchil, Tounfit, Tinjdad and Tinghir at 100,000). For the stratigraphic terms: 1. CAMP basalts and Triassic argillites; 2. the Lower Lias limestones; 3. Tassent Formation; 4. Bab n'Ouyad Formation. 5. Tislit Formation; 6. Imilchil Formation; 7. Isli Formation; 8. Tasraft Formation; 9. Quaternary deposits; 10. Jurassic-Cretaceous magmatic rocks; 11. Lakes; 12. Doleritic dykes; 13. Faults; 14. Anticlinal axis; 15. Synclinal axis; 16. Roads; 17. Studied synclines. **c** Synthetic log of all geological formations in the Imilchil area (modified after Charrière et al., 2011 and Ibouh et al., 2014)

This tectonic regime continued throughout the Late Jurassic to Cretaceous (Ouaskou et al., 2021). Compression and uplift of the entire Atlas system started in the Eocene and took place in compressive tectonic phases: The Late Eocene, Early Miocene and Pliocene–Quaternary phases (Frizon de Lamotte et al., 2008; Medina & Cherkaoui, 2021; Michard et al., 2011). The higher elevation of the High Atlas, compared to the Saharan and Tunisian Atlas, is mainly due to crustal shortening and mantle upwelling under the Atlas Mountains during the Neogene (Frizon de Lamotte et al., 2009; Fullea et al., 2010; Lanari et al., 2023; Miller & Becker, 2014; Teixell et al., 2003, 2014).

3 Material and methods

In examining the seismite beds within the Isli Formation, we adopted the methodology proposed by Owen and Moretti (2011) and Owen et al. (2011b) for investigating SSDS beds. This approach allows us to infer the palaeoenvironment of

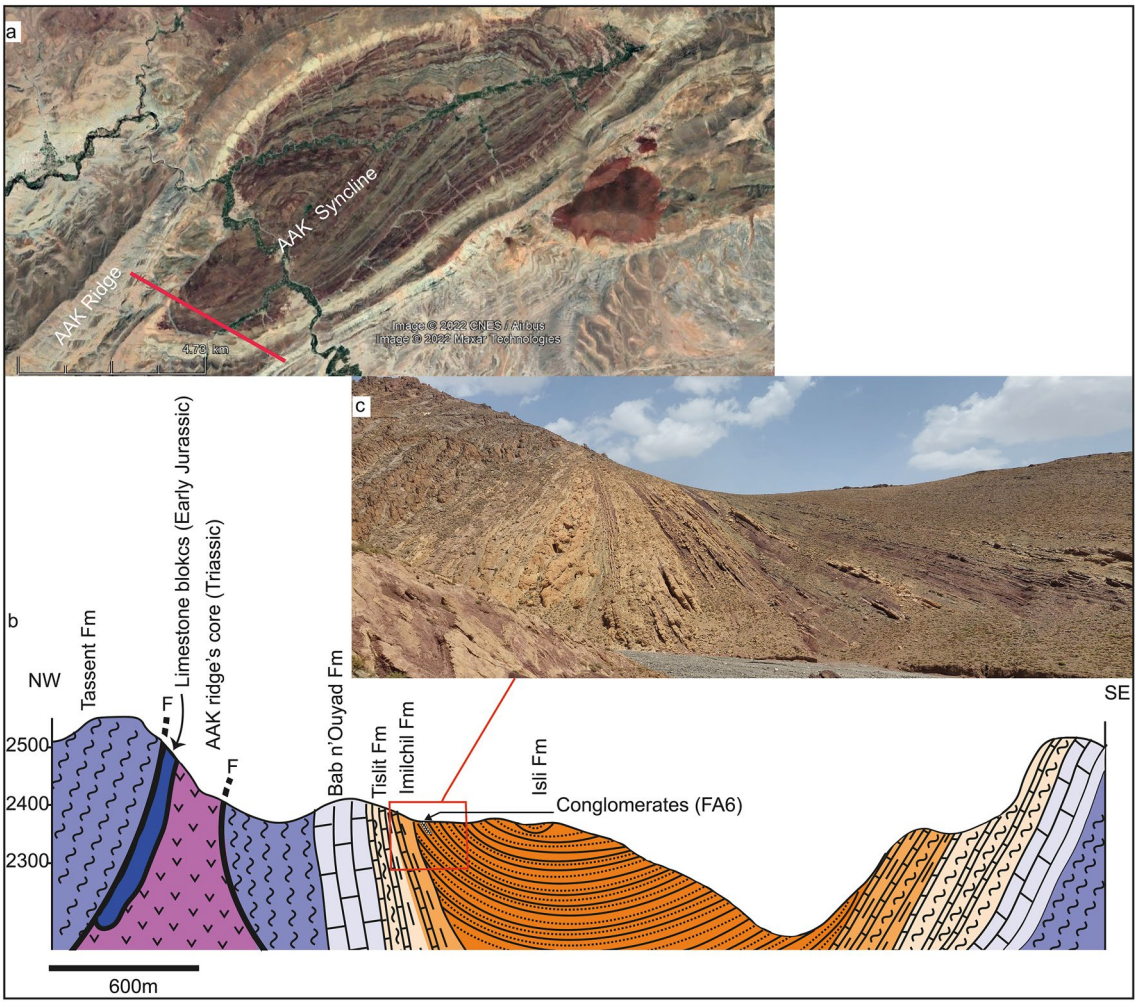

Fig. 2 A progressive unconformity in the AAK syncline. **a** Google Earth image showing the AAK syncline and the position of the structural section **b**. **c** A photo of the synsedimentary unconformity at the SW perisyncline termination

the deposits under study, using comprehensive field geological techniques including stratigraphy, petrography, facies analysis, and their associations. Furthermore, almost five hundred of loose and consolidated samples were collected and processed in the laboratory (washing for microfossils of charopytes and limnic ostracods and preparation of thin sections). For facies analysis, the classification of Miall (1978, 2006) for fluvial deposits and the classification of Flügel (2010) for lacustrine carbonates were adopted. The classification of SSDS is based mainly on their morphology and deformation style. Several different styles of nomenclature for SSDS have been developed in the literature. In the present paper, we adopted the classifications of Owen (2003), van Loon (2009) and Owen et al. (2011b). For interpreting the driving forces and deformation mechanisms, we employed the classifications of Lowe (1975), Owen (1987), and Owen et al., (2011a, 2011b). Concerning the triggers responsible for the deformation of the studied SSDS beds, we followed the most recent methodologies by Montenat et al. (2007), Owen and Moretti (2011), and Moretti and van Loon (2014). These methodologies provide suggested approaches for the recognition and correct interpretation of seismites.

4 Results

4.1 Stratigraphic position and sedimentology of the Isli Formation

The Isli Formation (lower Bathonian-? Late Jurassic) overlies the Imilchil Formation in the various synclines that were studied (Fig. 1b). The latter was dated to the upper Bajocian-lower Bathonian on the basis of brachiopods (Charrière et al., 2011). Unfortunately, the charophytes and ostracods collected in the Isli Formation have not enabled

us to establish a precise age. However, the upper marine beds of the Imilchil Formation have been dated to the Lower Bathonian using brachiopods (Ibouh, 2004; Oussou et al., 2023). Furthermore, the ichnoassemblage of the Isli Formation (Klein et al., 2023 and references therein) suggests that its age could extend to the upper Jurassic. This formation marks the beginning of the regressive phase in the High Atlas (Charrière & Haddoumi, 2017). The continental Isli Formation was deposited in a fluvio-lacustrine environment rich where dinosaurs, crocodilians and pterosaurs were common ichnofaunal components, as evidenced by their tracks and trackways (Gierliński et al., 2009, 2017; Klein et al., 2018, 2023; Oukassou et al., 2019; Boutakiout et al., 2020; Masrour et al., 2020; Ceniceros et al., 2022; Oussou et al., 2023). It consists of a succession of broad sandstone bars interbedded with thick red fine floodplain deposits and thick grey clay beds, which are mostly lacustrine. In addition, there are rare limestone beds in the Isli Formation that are rich in lamellibranchs, charophytes, freshwater ostracods, and limnic gastropods. The kilometre-scale sandstone bars contain fossil wood and show sedimentary structures such as planar cross stratification, horizontal laminations, raindrop imprints, and sometimes sedimentary structures of microbial origin.

4.1.1 Facies analysis and facies associations

In order to reconstruct the depositional environment of the Isli Formation, we logged a section in each of the three synclines studied (Fig. 3). The various facies types observed are described and placed in a palaeoenvironmental setting (Table 1 and Fig. 4).

To define the depositional environment of the Isli Formation, the facies observed are grouped into facies associations as described below.

Channel-belt facies association (FA1). This facies association is represented by a few isolated sandstone channels that are 2–5 m thick and about 30 m wide (Fig. 5a). The association is very rare in the formation (three in the Isli syncline, six in the AAK syncline and two in the Outerbat syncline). The facies of these channels are mainly fine to medium sandstones (Sm, Sp, Sh), sometimes interbedded with red siltstones (facies Fm) and other types of sandstone channels. The facies association is organised into thick sandstone bodies with planar erosive bases. It forms more or less tabular sandstone bodies and the boundaries of the facies are horizontal with lateral accretion dominating. The geometry of these channels is similar to that of the Salt Wash DFS median zones of the Morrison Formation in the USA (Owen et al., 2015). These channels are often embedded in floodplain and sheetflood deposits.

Isolated channel fill facies association (FA2). FA2 consists of multistory sandstone bodies (Sh, Sp, Sr and St), generally of medium grain size. These channels are between 4 and 25 m wide and between 2 and 7 m high. These isolated ribbon-like channel sandstone bodies with sharp erosive bases and centimetric intra-formational conglomerate beds (Gm facies) are multistory with maximum thickening along the channel axis and lateral thinning towards the edges. This association passes laterally to the unchanneled sheetflood deposits (single-story type; FA3). This facies association is generally associated mainly with the Fm and Stm facies (Fig. 5b) and have clear erosion surfaces, cutting through the floodplain deposits. Fossilized wood and dinosaur footprints are present in these sandstones. The sedimentary structures observed in this association (trough cross- and planar stratifications) indicate lateral migration of sandstone bars in fluvial channels. These sandstone channels are the result of multiple avulsions to distal areas (e.g., Klausen et al., 2014; Slingerland & Smith, 2004).

Sheetflood facies association (FA3). The sheetflood facies association is formed predominantly of very fine to fine sandstones and occasionally siltstones. These 0.2–1.5 m thick and kilometre-wide sandstones are organised in horizontally bedded layers (Fig. 5c). This association consists mainly of Sm, Sh, Sr, Sp, St and Sb facies. The surfaces of these tabular sandstone sheets contain features such as microbially-induced sedimentary structures (MISS) (sensu Noffke et al., 2001, 2022), raindrop marks and burrows. In addition, this facies association is very rich in fossil wood and dinosaur and tetrapod tracks, indicating a fluvial environment for this association. The association is interpreted as a sheetflood of the distal zone of a large distributive fluvial system (DFS) (e.g., Owen et al., 2015). These sandstone beds are laterally and vertically restricted mainly to fine floodplain facies.

Floodplain facies association (FA4). Facies of this association are the most dominant in the Isli Formation. FA4 is formed by thick and laterally continuous beds of red clayey siltstones (facies Stm, Fl, Fm, Stp) which extend for many km and are about 20 m thick (Fig. 5f). this facies association comprise also overbank and heterolithic splay deposits (Fig. 5e). FA4 is interbedded with either the sandstone channels of the FA1, grey argillites or lacustrine carbonates. Some immature palaeosols characterised by rhizoliths and calcrete nodules are present. These red siltstones sometimes contain intercalations of centimetre-scale beds of very fine sandstone and siltstones with carbonate cement. These intercalations are very rich in desiccation cracks, small current ripples and footprints of dinosaurs, mainly of sauropods. Some beds have yielded charophyte oogonia. These structures indicate temporary emersion. The horizontal laminae observed in these fine-grained facies indicate a very low energy sedimentation environment. This association corresponds to the large floodplains of a large fluvial system.

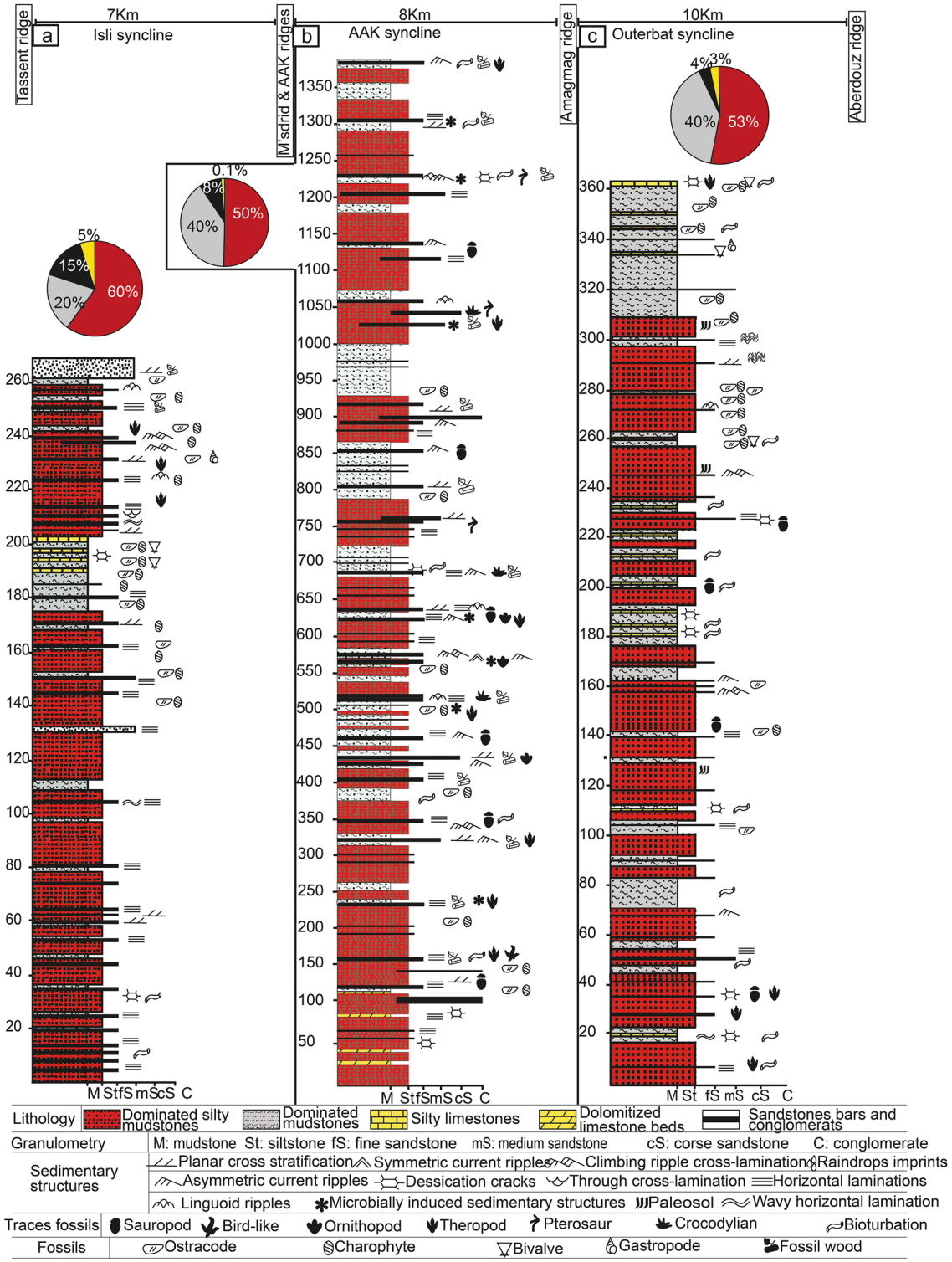

Fig. 3 Synthetic sedimentological logs of the Isli Formation in the three studied synclines. **a** Log of the Isli Formation in the Plateau des Lacs syncline, **b** Ait Ali Ou Ikkou (AAK) syncline, **c** Outerbat syncline. The circles beside each log indicate the percentage of different facies assemblages. The numbers 7, 8 and 10 km at the top of the figure correspond to the distance between the anticlinal ridges bordering different synclines of the area

Table 1 Facies description and interpretation of the Isli formation

Code	Facies	Bed thickness (m)	Description	Interpretation
P	Palaeosol (protosol). Figure 4g	0.2–0.3	Palaeosol horizons with white carbonate nodules and rhizoliths within the red clayey siltstone facies	Poorly developed soil with chemical precipitation
Ca	Calcrete. Figure 4g	0.2–0.3	Rhizoliths (Rhizogenic calcrete) and nodules of white limestone in palaeosol horizons	Secondary precipitation of carbonates, subaerial exposure and arid climate (Alonso-Zarza & Wright, 2010)
Fl	Silty claystone with v. small ripples and fine laminations. Figure 4i	Up to 0.1	Brick-red silty claystone with small millimetre-scale ripples, very fine laminations, desiccation cracks, bioturbation and dinosaur footprints. This facies is intercalated with thick layers of Stm facies	Overbank, abandoned channel, or waning flood deposits (Miall, 2006)
Stm	Clayey siltstone. Figures 4b, f and n	1–15	Brick-red, Massive, clayey siltstone, sometimes with fine horizontal laminations. This facies sometimes contains bioturbation, desiccation cracks, palaeosols and charophyte oogonia. This facies alternates with all the other facies	Sedimentation by settling in large floodplains. Colour, root traces and protosol indicate emersion
Mm	Claystone. Figures 4b, l	1–5	Grey, massive claystones, sometimes silty, with freshwater ostracods and/or charophytes oogonia and small gastropods. They sometimes contain fossil wood and horizontally laminated thin beds of siltstones	The association of osctracods and charophytes indicates sedimentation in a near-shore lake floor palaeoenvironment (Flügel, 2010)
Ms	Silty claystone with alternating sandstone. Figure 4l	1–3	Grey, red silty claystone with rhythmic alternation of centimetre-scale beds of finely laminated grey siltstone and sandstone. They contain ostracods, charophyte oogonia and gastropods. This facies is bordered by facies F, LMF and **S**	Low energy deposits, shallow lacustrine
Fm	Claystone with desiccation cracks	Up to 0.1	Beige claystone with desiccation cracks, bioturbation and sometimes sauropod footprints	Overbank, abandoned channel, or drape deposits (Miall, 2006)
Sh	Horizontally laminated sandstone. Figure 4a, h	0.15–1.5	Red, greenish, well sorted, fine to medium sandstone within mm-scale horizontal laminations and sometimes bedding. Fossil wood, bioturbation and dinosaur footprints are common on the surface. This facies is bordered by several other facies such as Sm and Stm	Plane-bed flow (critical flow) (Miall, 2006)
Sr	Sandstone with climbing ripple. Figure 4d	0.1–1	Red, brownish, well sorted, fine to medium to medium sandstone with a succession of climbing ripple cross-laminations	This type of facies indicates Ripples (lower flow regime) (Miall, 2006)
Sm	Massive sandstone. Figures 4a, l	0.1–0.4	Red, grey, massive, well-sorted fine to medium, sometimes silty, sandstone with fossil wood, microbially induced sedimentary structures (MISS), bioturbation, footprints and ripples on the surface	Sediment-gravity flow deposits (Miall, 2006)

Table 1 (continued)

Code	Facies	Bed thickness (m)	Description	Interpretation
Sp	Planar Cross-bedded sandstone. Figure 4e	0.2–1	Red, yellow, well sorted, medium to coarse sandstone within grouped planar cross-beds. This facies bordered usually by Sh and Sm and others facies of floodplains	Transverse and linguoid bedforms (2-D dunes). (Miall, 2006)
Sl	Low-angle palanar cross stratifications sandstone. Figure 4h	Up to 1.5	Yellow, red, well-sorted, fine to medium carbonate sandstone with low-angle (< 15°) planar cross stratification	Scour fills, humpback or washed-out dunes, antidunes. (Miall, 2006)
St	Trough cross bedding sandstone. Figure 4h	Up to 1m	Red, well sorted, very fine to medium sandstone with interlocking trough stratifications of about 20 cm. This facies is framed by red clayey siltstones (Stm) of the floodplains	deposition in lower flow regime of migrating 3D bedformes with sinuous crests
Sb	Bioturbated sandstone. Figure 4j	Up to 0.1	Very fine brownish sandstone, massive and well sorted. It shows intense bioturbation and desiccation cracks in its surface	Waning flow (lower flow regime) (Midwinter et al., 2017)
LMF9	Lamellibranch limestone. Figure 4m	0.3–0.5	White silty limestones very rich in freshwater lamellibranchs with charophyte oogonia and freshwater ostracods. This facies is intercalated with LMF2 and Lm facies	Sedimentation in a shallow near-shore lake (Flügel, 2010)
LMF2	Limestone with horizontal laminations. Figure 4n	0.15–0.90	Grey limestone with horizontal/wavy laminations. It shows traces of bioturbation and desiccation cracks. It is also affected by numerous structures such as small dykes, small slumps and loop bedding	Quiet water, lake offshore (Flügel, 2010)
Lm	Massive limestone. Figures 4f, n	Up to 1.7	Greyish, massive silty limestone with charophyte oogonia, freshwater ostracods and small gastropods. It sometimes shows desiccation cracks at the top, and is often limited by Stm, LMF2 and Mm facies	Shallow lake with emersive tendency
Stp	Pebbly muddy siltstone	Up to 0.1	Red, massive clayey siltstones with small sandstone elements and red siltstones form small channels interspersed within the floodplain deposits	Erosion and in situ reworking of sandstone and silty banks during floods
Gm	Sandy clast supported intraformational conglomerate	Up to 0.25	Composed of intraformational elements of red sandstone, grey limestone, fossil wood and red siltstones up to 1 cm in diameter with a sandstone matrix. They are in lenses and small channels often deposited directly on the erosion surfaces	High-energy reworking of the elements of the formation layers
Gmm	Matrix-supported extraformational conglomerate. Figure 4o	0.15–0.3	Greyish, medium-sorted subrounded breccia elements with predominantly Jurassic marine limestone elements of diameters $\phi = 2$–5 cm and fine-grained carbonate matrix	Erosion and reworking of the marine limestone of the neighbouring anticline

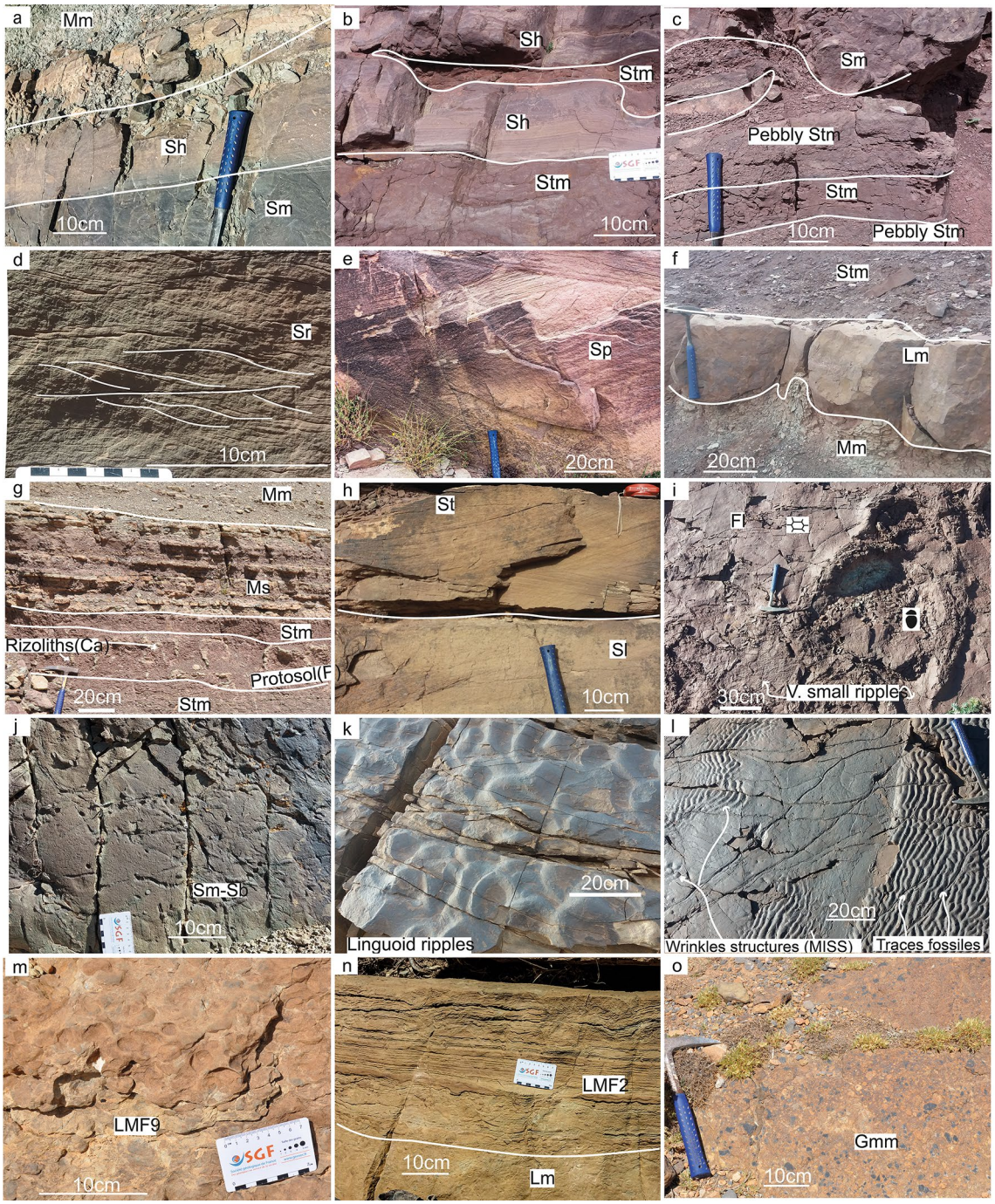

Fig. 4 Different facies of the Isli Formation: **a** Sm: massive fine sandstone; Sh: reddish fine sandstone with horizontal lamination; Mm: grey silty claystone. **b** Stm: massive clayey siltstones. **c** Red pebbly Stm. **d** Sr: fine sandstone with climbing ripples. **e** Sp: whitish carbonate sandstone with planar cross laminations. **f** Lm: massive silty limestone with charophyte oogonia, ostracodes, and gastropods. **g** Ms: silty mudstone interbedded with fine sandstone beds; calcrete rizoliths (Ca) in a palaeosol (protosol) bed (P). **h** Sl: sandstone with low-angle planar cross laminations; St: brick-red fine sandstone with trough cross laminations. **i** Fl: silty claystone with desiccation cracks, sauropod footprint, and small current ripples. **j** Sb: bioturbated fine sandstone. **k** Sandstone bed surface with linguoid ripples. **l** Massive fine sandstone with MISS and fossil traces **m** LMF9: lumachellic limestone with lamellibranchs. **n** LMF2: lacustrine limestones with horizontal laminations. **o** Gmm: matrix-supported conglomerates with mostly angular elements of a debris flow

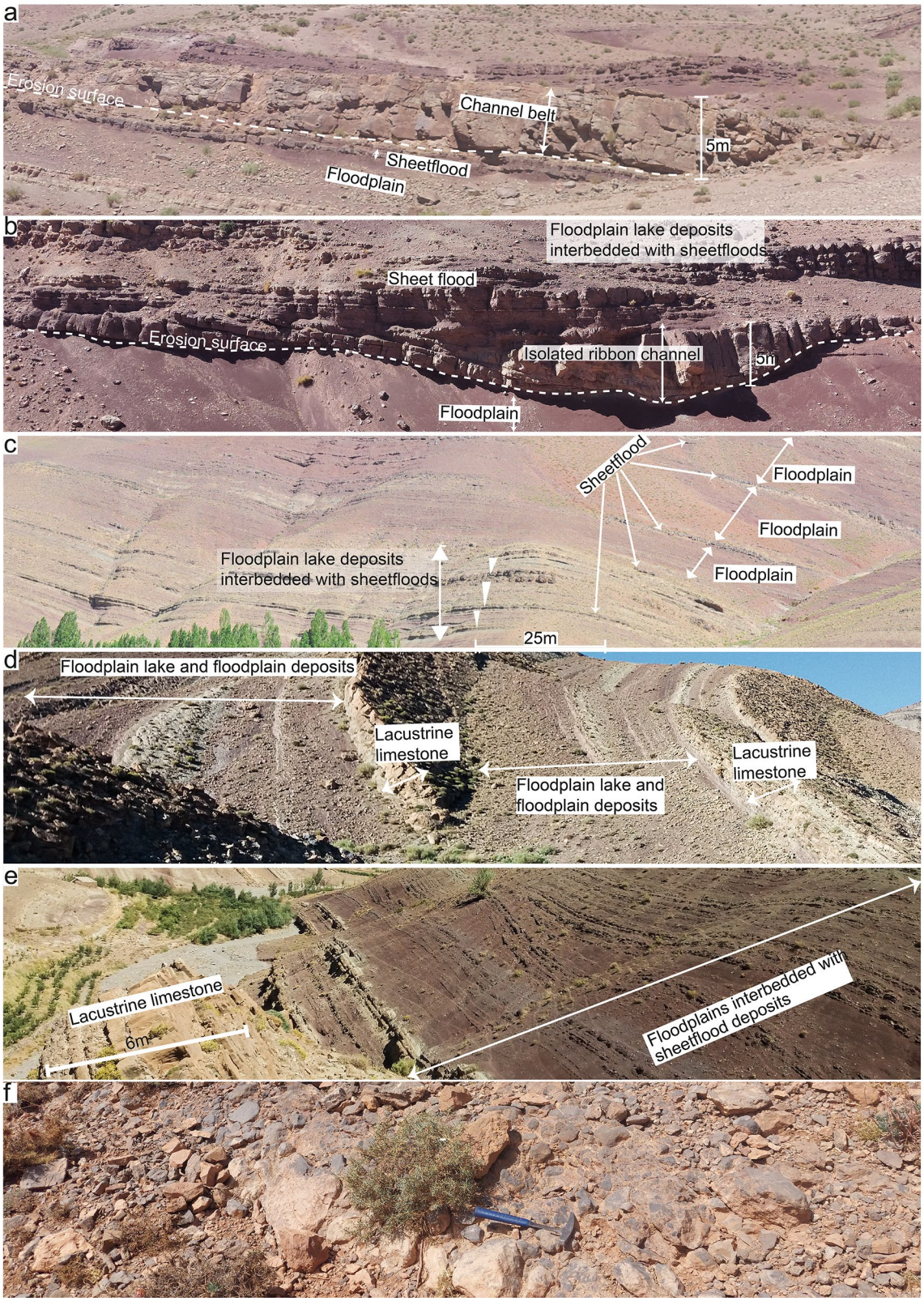

Fig. 5 General views of facies associations. **a** Outcrop of a sandstone channel-belt facies association (FA1). **b** Isolated (ribbon-like) channel-fill facies association (FA2). **c** and **d** Side views of the vertical succession of facies associations FA3, FA4 and FA5. **e** Close-up view of facies FA4 and FA5. **f** Surface view of part of the extraformational conglomerates of the debris flow facies association (FA6)

Lacustrine facies association (FA5). This association is formed by limestone beds associated with massive and sometimes laminated grey silty clays and mudstones (Fig. 5c–g). The limestones are represented by lamellibranch lumachelles, laminated limestones and massive limestones, with ostracods and charophyte oogonia. Some limestone beds are bioturbated and show desiccation cracks, indicating subaerial exposure. The grey mudstones contain ostracods, gastropods and charophyte oogonia, as well as fossil wood. Facies Lm, LMF2, LMF9, Ms and Mm are very common and extend for several hundred metres, especially in the Outerbat syncline. Non-carbonate facies were deposited in lake floodplains, small siliciclastic lakes or ponds. This association is bordered by facies of FA3 and FA1.

Debris flow facies association (FA6). The debris flow facies association has a relatively small outcrop area of about 40 m^2 and a thickness of slightly more than 3 m in the southwestern periclinal termination of the AAK syncline. It consists mainly of massive conglomerates with an incised base (Gmm facies, Table 1, Figs. 4o and 5f). These extraformational conglomerates, which are organised in layers interbedded with siltstones and argillites similar to the rest of the formation, are formed by centimetre-scale elements of local origin, mainly marine carbonates derived from the neighbouring ridges. Palaeogeographically, this facies association suggests that part of the Jurassic marine carbonate cover of the AAK ridge was already in place and was eroded during sedimentation of the Isli Formation.

4.2 Depositional Palaeoenvironment of the Isli Formation

The presence of sandstone channels of different types, facies, and geometries, fossilized wood, raindrop marks, and dinosaur and crocodilian footprints together indicate that the Isli Formation is continental. This is supported by the presence of lacustrine and floodplain deposits with charophyte oogonia and limnic ostracods. There is no evidence of marine deposition in the Isli Formation.

In accordance with Miall's (2006) criteria, (i) the presence of facies St, Sh, Sl, Sr, Fl and Fm, (ii) the rarely channelised sandstone bodies intercalated with clayey argillites and siltstones, (iii) the presence of aridisols and calcretes (nodules and rhizoliths), and (iv) the abundance of mud cracks on the surface of the beds, may indicate a warm climate with arid trend. The presence of fossil wood in the sheetflood facies could be explained by its transport from upland areas during flooding.

The very large length/width ratio (L/H ratio) of the sheetflood sandstones (FA3), the rarity of the channel-belt facies association deposits (FA1), the abundance (more than 75%) and thickness (sometimes more than 15 m) of the floodplain and lacustrine deposits, and the dominance of fine and very fine grain sizes in almost all sediments indicate that these sediments are distal. Therefore, the depositional environment corresponds to a distal zone of a Distributive Fluvial System (DFS) according to the criteria of several authors (Hartley et al., 2010; Nichols & Fisher, 2007; Owen et al., 2015; Plink-Björklund, 2021; Weissmann et al., 2013). In this distal zone, lacustrine deposits may be associated with detrital facies in the format of fluvio-lacustrine sequences. The extraformational conglomerates of low extension debris flow of local origin (< 1% of the formation) outcrop locally at the perisynclinal termination of the AAK syncline. These conglomerates indicate active growth of the AAK ridge during the deposition of the Isli Formation.

The DFS concept was first applied to the Isli Formation by Joussiaume (2016) in his study on diapirism in the region, although he did not rigorously analyse the whole formation. Joussiaume (2016) concluded that the proximal zone of the DFS was about 100 km to the west, in accordance with the eastward migration of a shoreline from the Jurassic sea during the sedimentation of the Isli Formation (Elmi, 1999 in Frizon De Lamotte et al., 2009). The distal zone of a DFS is a suitable area for the formation of SSDS as well as for the validation of certain seismite recognition criteria. This can be explained as follows: (i) the fine to very fine grain size (clay, siltstone and fine sandstone) favours liquefaction and liquidisation phenomena and (ii) the lateral extension of the sedimentary layers, on the order of several hundred metres, reflects the large extension of water and the saturation of the sediments over long periods of time (e.g., Obermeier, 1996).

4.3 Description and interpretation of soft-sediment deformation structures

Several beds with soft-sediment deformation structures have been identified in the three synclines of the Imilchil area. The studied formation also shows a wide variety of SSDS (Fig. 6), namely: neptunian dykes, plastic intrusions, load structures (load casts and pseudonodules), slumps, convolute lamination, water-escape structures (injection dyke and cusps), loop bedding, gravifossums and synsedimentary faults. In order to determine the driving forces of this deformation, the deformation mechanism and to deduce the triggers of these SSDS, we relied on sedimentological evidence, the depositional environment and the regional tectonic context, following the approach of Owen et al. (2011b) and Moretti and van Loon (2014). It is worth noting that the SSDS beds described in this work are produced by the same trigger. SSDS left by dinosaur locomotion (dinoturbation) are not considered here.

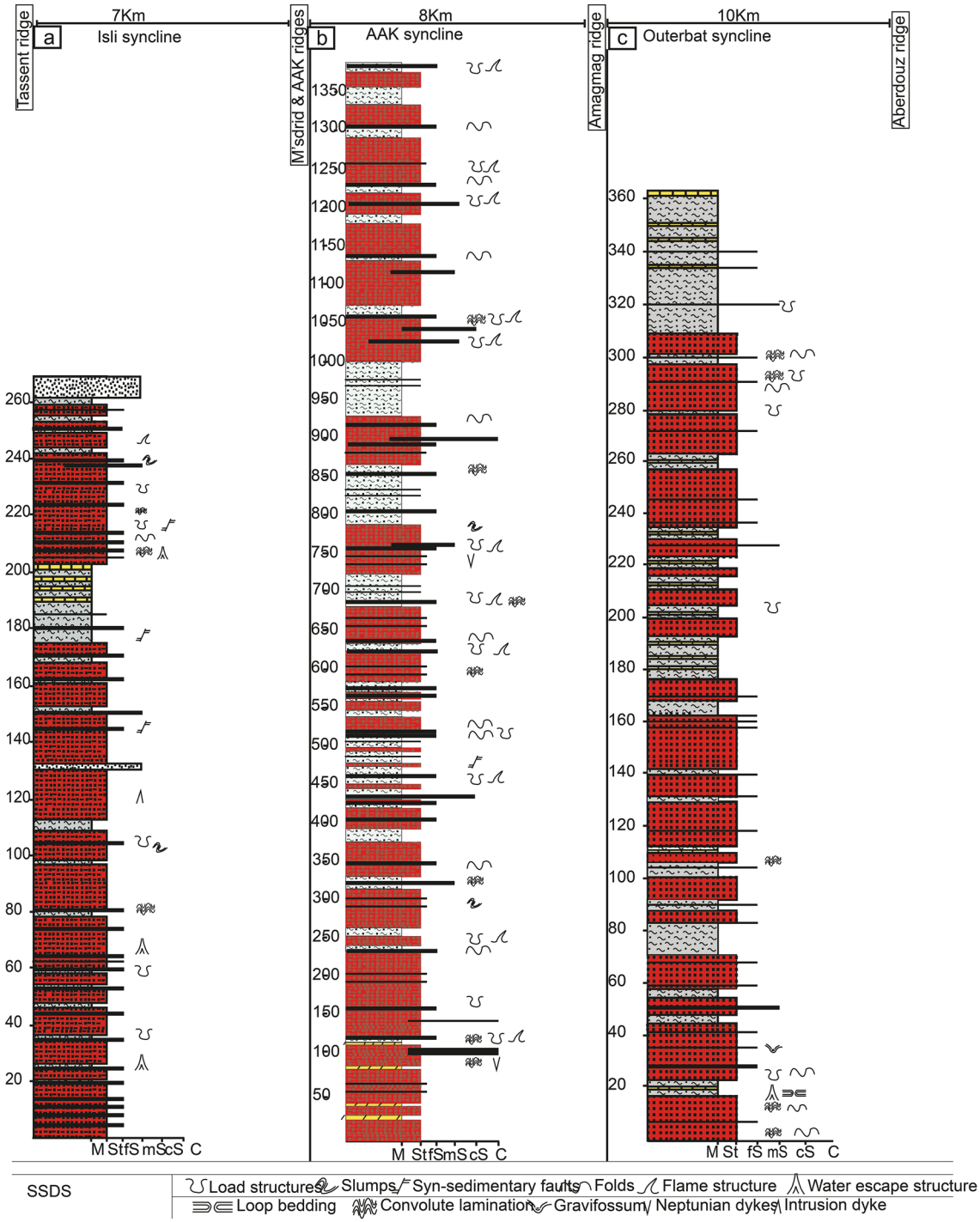

Fig. 6 Representative sedimentological logs with soft sediment deformation structures

4.3.1 Neptunian dykes

Description. Numerous neptunian dykes are well exposed within floodplain siltstones (Fig. 7a), in sheetflood deposit facies association (Fig. 7b, c) and also in lacustrine limestones (LMF2 facies). They are related to simple fissures 1 m to 2 m high and between 10 and 20 cm wide, with a downward thinning. These dykes are infilled by the fine sandstones and silty mudstones of the source layers and intruded the underlying floodplain and lacustrine facies.

Interpretation. The formation of neptunian dykes is preceded by nearly vertical fissures which open upwards.

Subsequently, sediment from the liquefied source layers fills these fissures. The host layers appear sufficiently consolidated to be fractured. In the absence of evidence of sedimentary origin, these structures would be the result of extensive brittle deformation (e.g., Montenat et al., 2007; Moretti & Sabato, 2007). The dykes observed in lacustrine limestones lack a regular shape, so they could be formed by karstic dissolution (Zeng et al., 2018), as these limestones are characterised by desiccation cracks on their surface.

4.3.2 Plastic intrusions

Description. Plastic intrusions (also known as 'hydrostatic intrusion' (Lowe, 1975) form clusters of fine material that cut vertically upwards and sometimes laterally through host beds. These structures are observed mainly in siltstone, claystone and fine sandstone beds. The observed structures have different dimensions, ranging from 20 to 30 cm high and 10 to 60 cm wide. Some of them are embedded between fine sandstone beds and form sills (horizontal intrusions) (Fig. 8a, b), others rise upwards within the host layers and form sedimentary 'diapirs' (Fig. 8c, d).

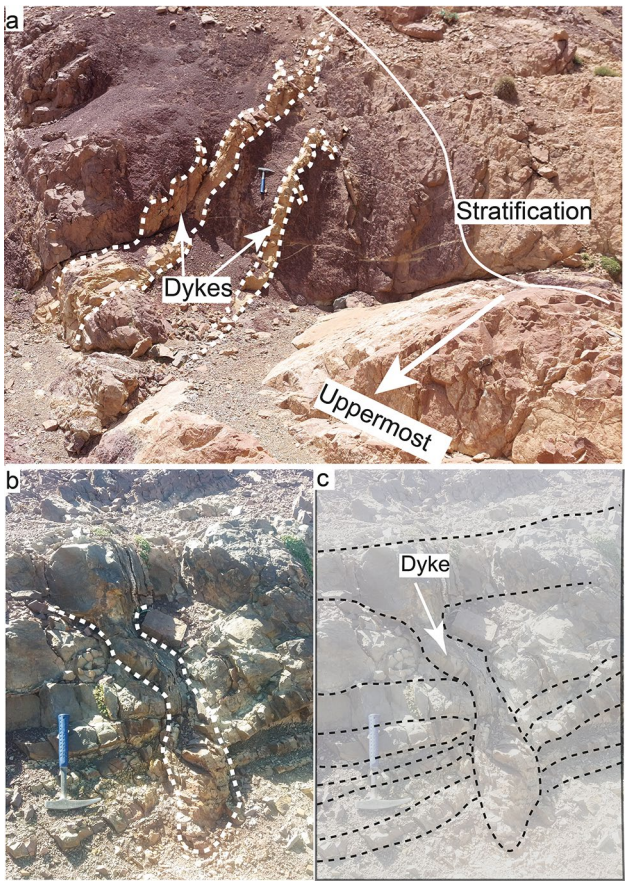

Fig. 7 Neptunian dykes. **a** Two neptunian dykes with material derived from lacustrine silty limestones descending into floodplain clayey siltstones. **c** Photograph. **d** Sketch of **c**. A neptunian dyke in sheetflood facies sandstones penetrating into underlying grey silty mudstones

Interpretation. These intrusions affect claystones and siltstones. Their geometric shapes are irregular, which distinguishes them from dykes. The upward movement of intrusion material is characterised by upturned bedding and also by bed separation in the case of concordant intrusions (sedimentary sills, e.g., Onasch & Kahle, 2002). These intrusions correspond to the vertical and lateral hydroplastic flowage of non-cohesive water-saturated sediments (Lowe, 1975) of the Mm and Stm facies into very fine sandstones (Sm and Sh facies). Similar deformational structures have been reported by many authors (e.g., Onasch & Kahle, 2002; Berra & Felleti, 2011; Suter et al., 2011; Lunina & Gladkov, 2016).

4.3.3 Load and associated structures (Figs. 6, 9)

Sedimentary beds with load structures outcrop, like the other SSDS, in all three synclines, but are most abundant in the AAK syncline, given the thickness of the formation there (> 1400 m), and its abundance of sandstone and silty bars intercalated with beds of predominantly Mm and Stm facies. More than 10 beds were observed in the AAK syncline, three in the Plateau des Lacs syncline and three in the Outerbat syncline. The structures observed are diverse and of different sizes. According to the classification of Owen (2003), we recognize the following five types: simple load casts, pendulous load casts, attached load casts, detached load casts, and ball and pillows. Other structures are also associated with load casts such as diapirs and flame structures. These structures are centimetres to metres in size and often occur at the interface between fine sandstones and grey siltstones or mudstones.

4.3.3.1 Load casts and flame structures Simple load casts. Simple load cast structures are observed at the base of numerous fine sandstone beds (Sh and Sm facies) of the sheetflood deposit facies association (source layers), penetrating the grey silty mudstones (Mm facies) of the lower layers (matrix). They form sandstone lobes, with sizes between 20 and 50 cm (Fig. 9a, b), which widen towards the source layer, while the silty claystones of the underlying lower layer form flame structures that thin upwards.

Pendulous load casts. At the interface between the fine, medium and sometimes coarse sandstone layers (Sm and Sh facies) and the underlying silty mudstone, pendulous load cast structures (Fig. 9c, d) are present. They are larger than the simple load casts and vary in size from 30 to 50 cm high and 10 cm to 50 cm wide. These structures have a shape that widens towards the bottom, where they are surrounded by the sediments of the lower layer (matrix).

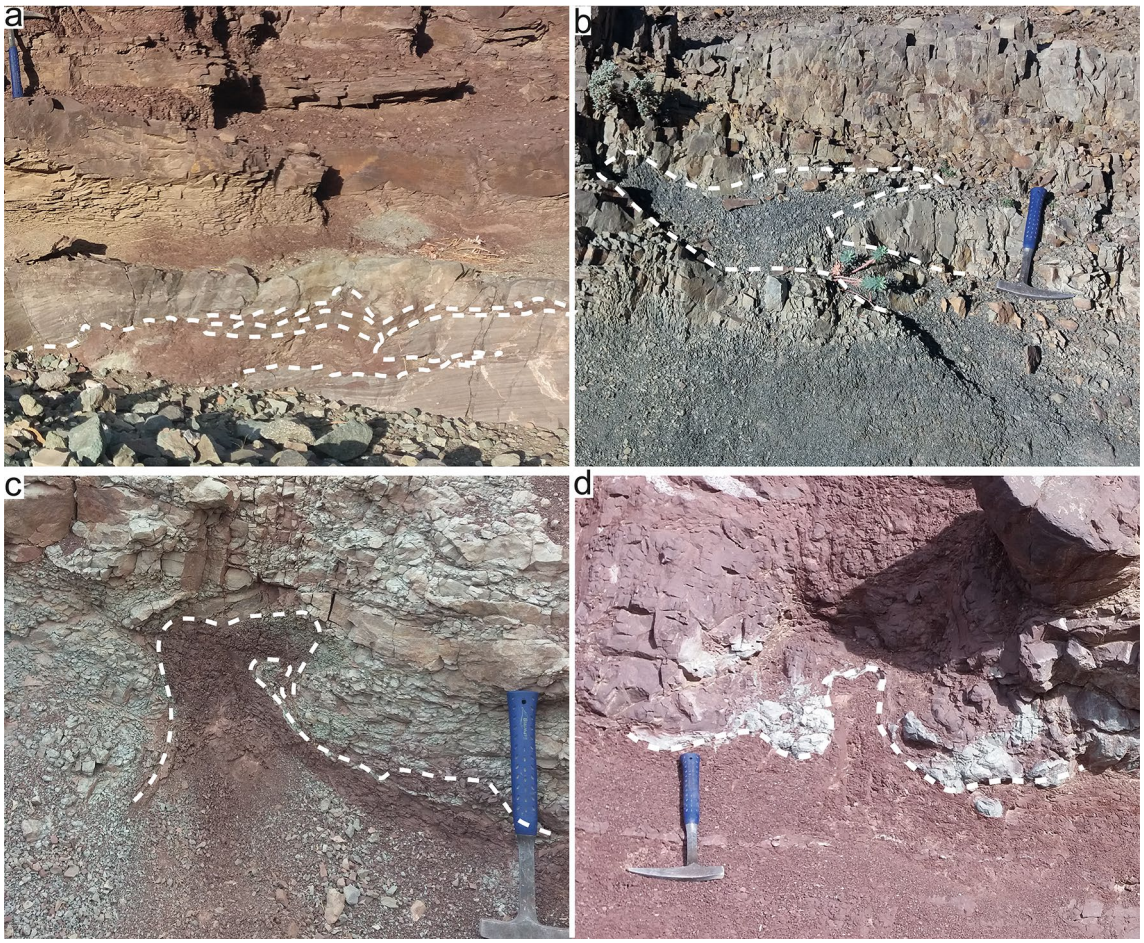

Fig. 8 Some field photos of the plastic intrusions. **a** A sill of clayey siltstones in fine sandstones (Sh). **b** A sill of grey siltstone in fine sandstone. **c** The vertical intrusion of red siltstone into grey siltstone. **d** The vertical intrusion of red siltstone into very fine sandstone

Flame structures. Flame structures form 'anticlines' between simple load casts and pendulous load casts along the interface of the two deformed layers (Fig. 9a–d). These are often grey silty clays, which rise upwards forming sharp anticlines in the case of simple load casts, and broaden upwards in the case of pendulous load casts. The sediments of the flame structures are sometimes eroded, leaving cavities between the simple and pendulous load casts (Fig. 9c).

4.3.3.2 Interpretation of load casts and flame structures The beds affected by the load casts and flame structures formed, according to Rayleigh–Taylor instability, when the two mobilised layers are liquefied (Owen, 1987, 2003). Owen also attributed the formation of these structures to gravitational forces associated with the reversed density system of Anketell et al. (1970). The beds affected by these structures consist of alternating silty mudstones and fine to very fine sandstones which favour fluidisation (Allen, 1982; Lowe, 1976). The formation of simple load casts and pendulous load casts depends on the rate of liquidisation of the sedimentary layers and the continuity of the deformation. Within the Isli Formation, pendulous load casts are the most developed form of load cast structures.

4.3.3.3 Pseudonodule structures Attached and detached pseudonodule structures. At the interface between fine sandstone and silty claystone, many deformed beds contain pseudonodules, which are either attached (Fig. 9e, f) or detached (Fig. 9g) from their source layers. These pseudonodules are of different sizes, 30–60 cm wide and 0.4–1 m high, and are surrounded by the sediments of the lower layers (matrix), often grey silty mudstones. In some cases, the matrix layer shows deformation, such as small faults and folds, caused by the downward movement of the pseudonodules (Fig. 9e). Some detached pseudonodules are characterised by primary laminations preserved despite movement towards the matrix layer (Fig. 9g).

Ball and pillow structures. These structures are formed by balls of coarse siltstones and well compacted fine sandstones (Fig. 9h, i). They are rounded in shape, have

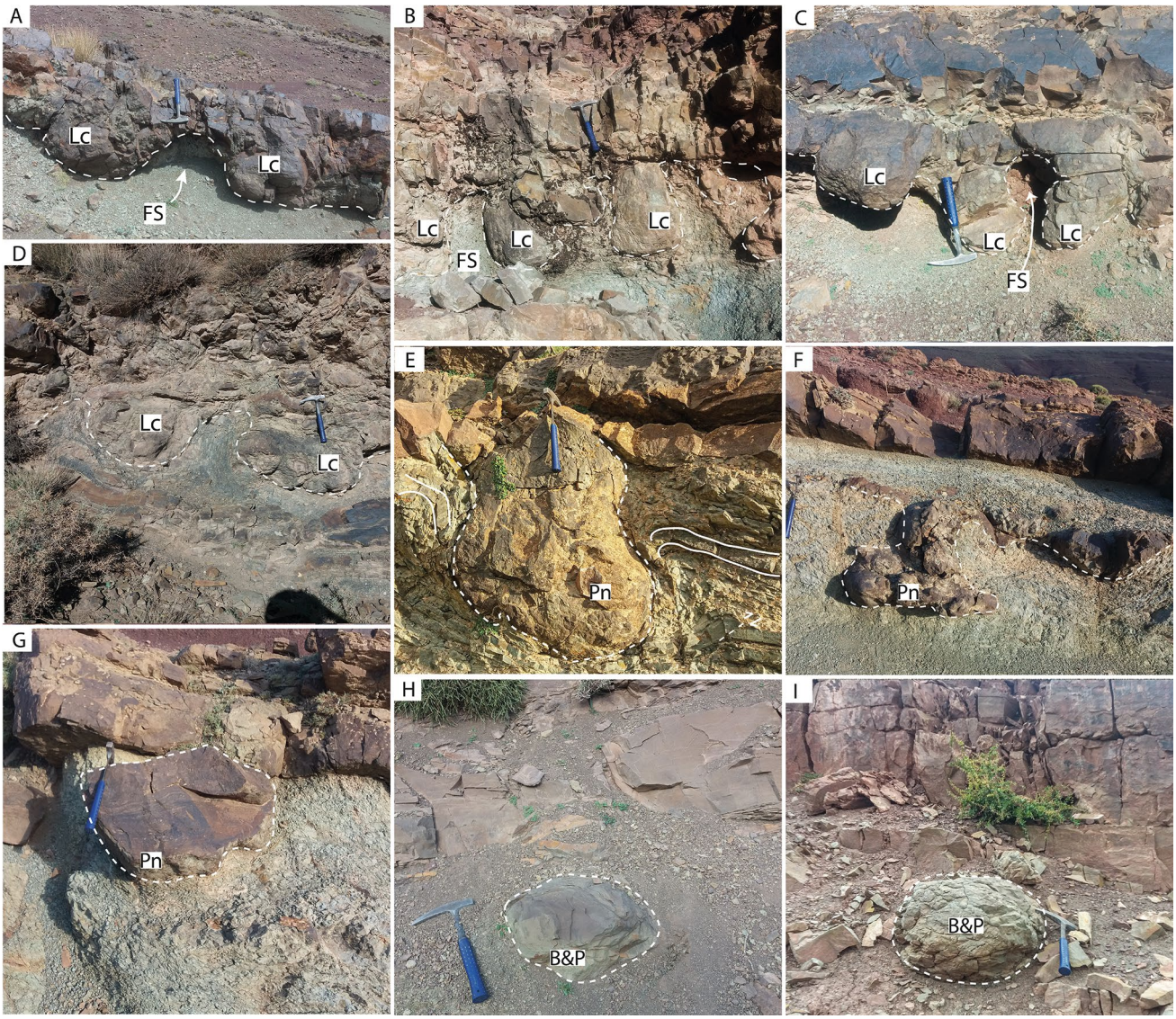

Fig. 9 Field photos of some load structures. a Simple load casts (Lc) with flame structures (FS) in the interfingering of a sheetflood sandstone bed and a lacustrine silty mudstone. b and c Pendulous load casts (Pn) with upward open diapirs in the same facies as A. d Pendulous load casts with folded deformation below the matrix and small load casts in the source layer above the main deformed bed. e A large attached isolated pseudonodule caused folding and faulting (bottom right) in a more-or-less lithified matrix during deformation. f Attached pseudonodule rooted in silty claystone. g Detached pseudonodule with preserved horizontal laminations (Sh facies). h and i Ball and pillow structures (B&P) are formed by fine sandstones preserved in silty mudstones. Hammer for scale (33 cm)

a diameter of about 35 cm, and are completely detached from their source layers. They are buried in the underlying matrix, which is composed of grey lacustrine clays and red siltstones. This type of load structure is observed in the Plateau des Lacs and in Outerbat synclines.

4.3.3.4 Interpretation of pseudonodule structures The mode of formation of these structures is the same as that of the load casts, already described above, except that it is more advanced in terms of the degree of deformation at the ball-and-pillow bed (Owen, 2003). Owen attributed this mode to the repeated detachment of pseudonodules contemporaneously with continuous fluidisation, as well as to the very high density of the source layer compared to the matrix, implying a downward movement of the sandstone balls within the silty argillites. Pseudonodule structures are widely reported from diverse depositional environments (e.g., Sims, 1975, 2013; Berra & Felleti, 2011; Koç-Taşgın, 2011; Pillai & Kale, 2011; Liesa et al., 2016; Ali & Ali, 2018; Morsilli et al., 2020).

4.3.4 Slumps

Description. Slumps of varying sizes, ranging from centimetre to decimetre-scale, occur in the Isli Formation sedimentary beds (Fig. 3). These slumps are well preserved within sheetflood sandstones (Fig. 10a-c), floodplain deposits (Fig. 10d) and lacustrine limestone (facies) (Fig. 10e). The slump sheets are always intercalated with undeformed beds, with some of them are characterised by single fold, while others extend continuously over a few meters' length with symmetrical, asymmetrical and sub vertical axial planes folds. They affect the entire bed, but sometimes the deformation only affects its basal part (Fig. 10b).

Interpretation. The intercalation of slumps and undeformed sedimentary beds indicates that they are SSDS (Alsop et al., 2019, 2020; Collinson & Mountney, 2019; Maltman, 1984; van Loon, 2009). However, distinguishing between folding during soft sediment deformation (SSD) and tectonic folds in the sedimentary record is quite a delicate task (see Maltman, 1994; Waldron & Gagnon, 2011; Alsop et al., 2019, 2020).

During slumping, a single event occurs for each slump bed, which is formed by the gravity-driven shearing of partially liquefied beds (e.g., Alsop & Marco, 2013). The affected beds are quasi-horizontal and there is no evidence of a slope, but this does not prevent their formation. It is known that these structures form on slopes of less than 1° (García-Tortosa et al., 2011) and potentially even less than 0.25° (Spalluto et al., 2007). Thus, oversteepening can be ruled out for the formation of these slumps. Several authors have described similar slumps as SSDS (e.g., Martín-Chivelet et al., 2011; Spalluto et al., 2007).

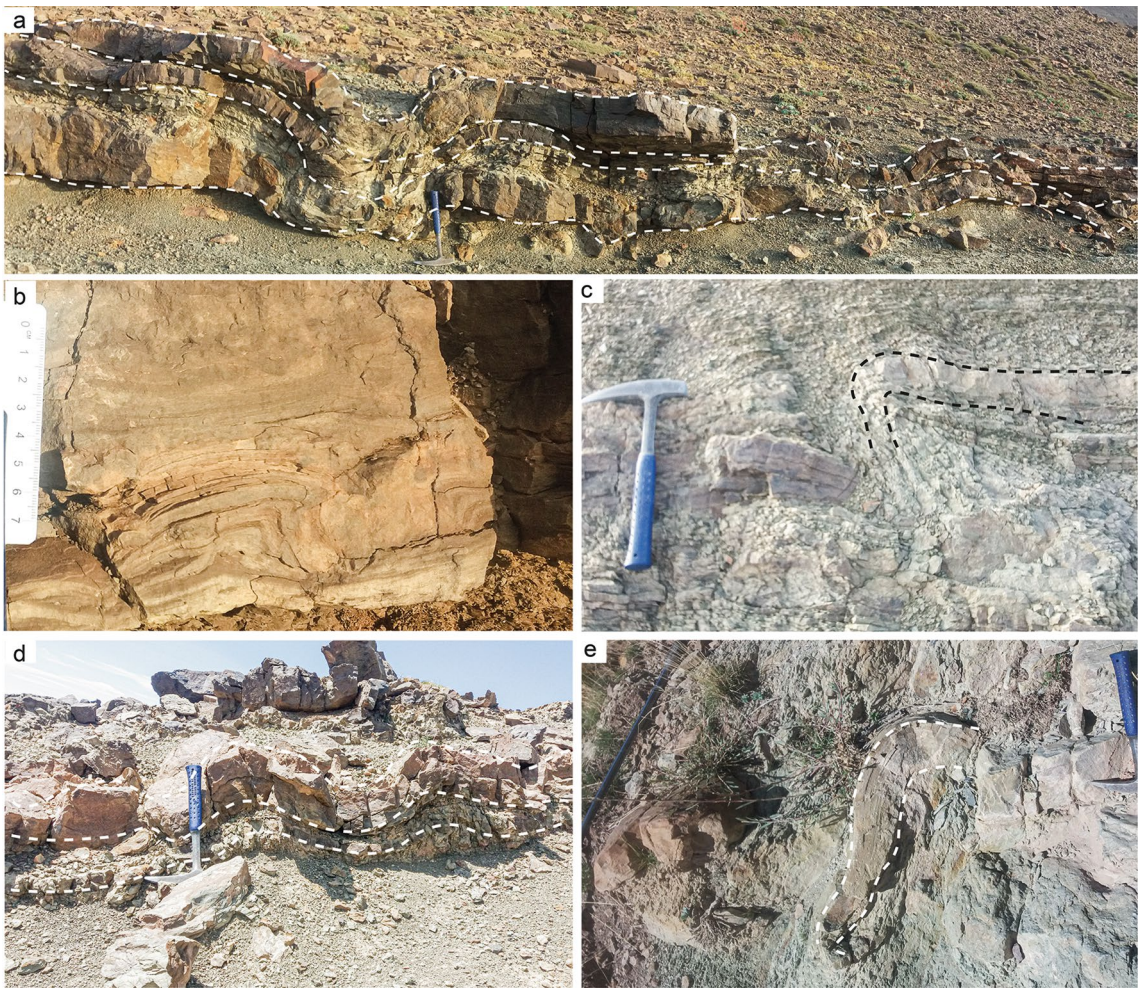

Fig. 10 Examples of slump folds exposed within some sedimentary beds. **a** Continuous slump folds within sheetflood sandstone. **b** The slump in horizontally bedded sandstones (Sh facies) with axis plane N145 and inclined to the southeast. **c** Slumping in the siltstone interbedded with fine sandstone. **d** The slump in the siltstone interbedded with fine sandstone. **d** Hydroplastic anticlinal and synclinal folds in the sandstones (Sh facies)**. e** soft sediment folding in lacustrine limestone

4.3.5 Convolute laminations

Description. In a bed, deformed laminations bounded by undeformed laminations are called convoluted laminations (Allen, 1977, 1982). Convolute laminations described here are up to 15 cm high and sometimes extend laterally for a metre or more. In the Outerbat syncline, beds of lacustrine silty limestone contain slightly folded laminae (Fig. 11a). Sometimes the laminations form asymmetrical folds, especially in fine to medium horizontally laminated sandstones (Sh facies) (Fig. 11b–d). Laminations also show anticlines with an upward increase in amplitude (Fig. 11c, d). Some convolute laminations occur in beds that also exhibit load structures.

Interpretation. This type of SSDS is widely described in different environments and several interpretations have been proposed. For example, Neuwerth et al. (2006) concluded that convoluted laminations are due to gravitational instabilities associated with inverse density gradients. Structures found in the sheetflood deposit facies resemble those described by Davies et al. (2005), who concluded that convolute laminations are due to the formation of anticlines and synclines in the upper parts of the liquidised beds. Otherwise, these structures are formed when the cohesive strength and low permeability of the accumulated sediments begin to prevent escape of the free upward flow of pore fluids (Lowe, 1975). According to Moretti and Sabato (2007), convolute lamination structures are only formed in sandstone and silty sediments due to liquefaction.

4.3.6 Water-escape structures

4.3.6.1 Cusps Description. Water-escape structures are well exposed in lacustrine limestones and sandstone facies of sheetflood deposits. These structures are small anticlinal cusps within the same bed, i.e. a group of laminae only which are involved in their formation. Their size can be up to 10 cm high and 6 cm wide. The upward movement of the material is clearly visible in the affected beds, pushing the crossed laminae upwards (Fig. 12).

Interpretation. As their name suggests, these water-escape cusp structures are formed when liquefied sediment flows upwards through the overlying laminae immediately after deposition (Ghosh et al., 2012). We distinguish them from plastic intrusions by their size and the sediments they affect. Fluidisation phenomena are well pronounced due to the vertical movement of the sediment (Lowe, 1976; Nichols et al., 1994), and this upward movement generates shear stress in the upper laminae according to fluidisation rate. Furthermore, the laminae through which the liquefied

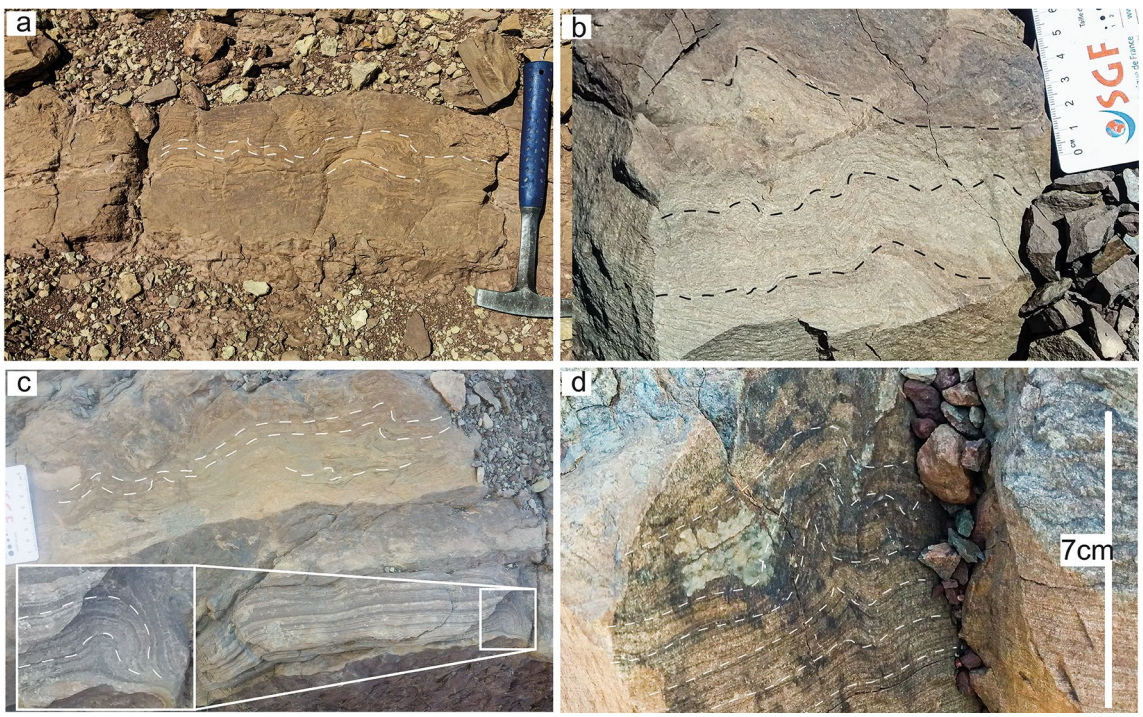

Fig. 11 Some convolute lamination structures observed in the different synclines. **a** Convolute laminations in gently folded folds in the lacustrine limestones (LMF2 facies). **b** Convolute laminations superimposed with asymmetric folds. **c** Convolute lamination with asymmetric open folds at the bottom and gently inclined syncline and anticline folds. **d** Folded lamination within the fine sandstone bed with a visible increase in amplitude towards the top

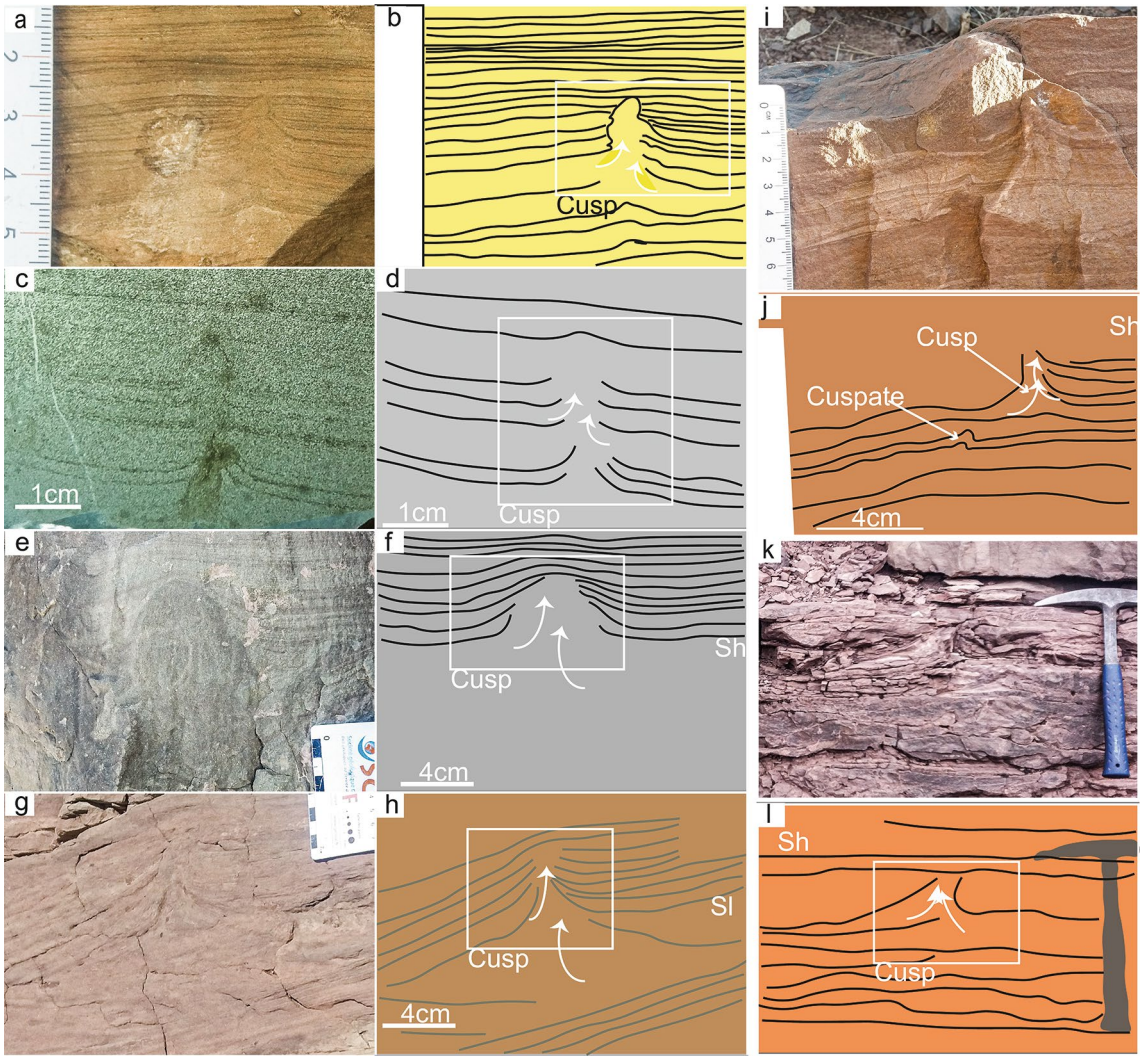

Fig. 12 Field photos and interpretation of water-escape cusp structures: **a** Photograph. **b** Sketch of **a**. water-escape cusp in lacustrine limestone (LMF2 facies). **c** Photograph. **d** Sketch of **c**. A silty mudstone cusp observed at the bed of the thin section (LMF2 facies). **e** Photograph. **f** Sketch of **e**. Cusp structure in a sandstone bed (facies Sh). **g** Photograph. **h** Sketch of **g**. a cusp in fine sandstone (facies Sl). **i** Photograph. **j** Sketch of **i**. Small, gently inclined anticlinal cusp. **k** Photograph **l** Sketch of **k**. Cusp structure in the fine sandstone (facies Sh)

sediment passes are less dense than the source laminae. This is the normal density gradient of Anketell et al. (1970). Often small folds in laminae less affected by liquefaction are the result of hydroplasticity and the localised development of fluidisation (Bhattacharya & Bandyopadhyay, 1998; Owen, 1996). Many similar water-escape structures are described in the related literature (Alfaro et al., 1997; Koç-Taşgın & Türkmen, 2009; Koç-Taşgın et al., 2011; Kundu et al., 2015; Rudersdorf et al., 2015; Ozcelik, 2016; Koç-Taşgın, 2017).

4.3.6.2 Injection dyke Description. A single intrusive dyke has been identified in the Isli Formation in the Plateau des Lacs syncline. It is 3 m high, 90 cm wide at the base and 40 cm wide at the top (Fig. 13). It consists mainly of white carbonate sandstones vertically cut by red clayey siltstones. The latter are formed by poorly consolidated floodplain siltstones. The whole structure is tilted towards the NE and affected by faults that have displaced the dyke itself. The sediment infill of the dyke is identical to that of an underlying layer, which is about 1 m thick, and may be the source layer. No primary sedimentary structures (such as laminations) are preserved in the dyke.

Interpretation. The similarity of the sediments infilling the dyke to those of the underlying source layer and the thinning of the dyke upwards demonstrate that it is an injection dyke. This type of dyke, recognised as a soft-sediment deformation structure (Montenat et al., 2007), results from a fluidisation process by raising pore pressure, which allows

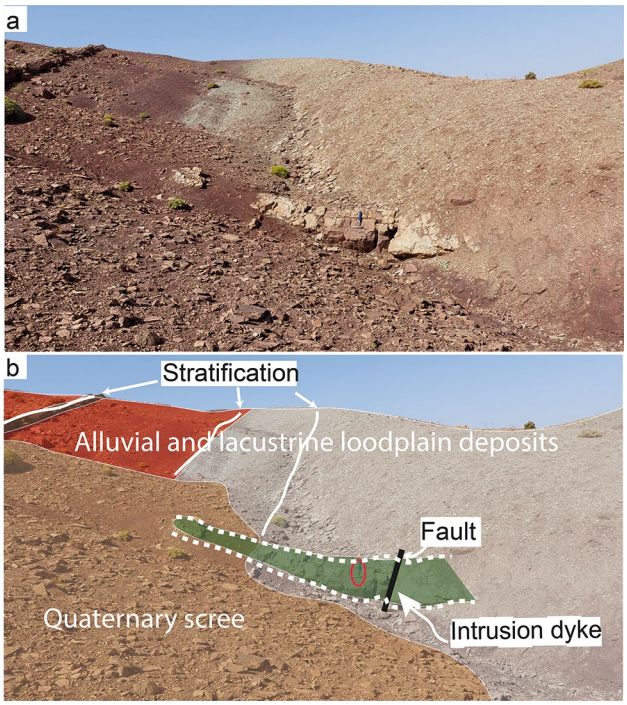

Fig. 13 A Photograph. Sketch of **b.** Injection dyke formed by carbonate sandstone shows upward thinning. Geological hammer for scale is 33 cm long (red circle)

the still water-saturated (liquefied) material to rise upwards through hydrofractures (Allen, 1982; Owen, 1996; Obermeier, 2009). This structure is widely described in different depositional environments (e.g., Obermeier et al., 1996; El Taki & Pratt, 2012; Ghosh et al., 2012).

4.3.7 Loop bedding structures

Description. Loop bedding structures (sensu Calvo et al., 1998), also called pinch-and-swell structures (e.g., Knaust, 2002) are a group of clearly stretched laminae with looped intervals. These structures are well exposed in a lacustrine limestone bed (LMF2 facies) in the Outerbat syncline. They are characterised by small stretched loop bedding of 1–3 cm associated with disturbed laminations, as well as thickening and thinning of lamina sets (Fig. 14a, b). Laterally in the same bed, loop beddings affect several superimposed laminae (Fig. 14c) and are sometimes associated with neptunian-like dykes (Fig. 14d).

Interpretation. Like other SSDS, these structures are formed during sedimentation before the sediment is fully lithified. They are formed in beds that are sensitive to hydroplastic behaviour, and they result from horizontal stretching parallel to the laminations (Plaziat & Ahmamou, 1998; Calvo et al., 1998; Knaust, 2002). This stretching is due to local normal stress. This type of soft-sediment deformation structure has been reported from different geological settings by Calvo et al. (1998), Rodríguez-Pascua et al. (2000), Berra and Felleti (2011), Martín-Chivelet et al. (2011), El Taki and Pratt (2012), Dechen and Aiping, (2012), Törö and Pratt (2016), Yang and van Loon (2016), Zeng et al. (2018), Chen et al. (2020) and Alencar et al. (2021).

4.3.8 Gravifossum structures

Description. In the Outerbat syncline, two gravifossum structures (sensu van Loon & Wiggers, 1976) were observed. These are two small depressions. The first one, which is 1 m wide and 0.6 m high, affects clayey siltstones and fine sandstones and is filled with grey silty mudstones and fine sandstones (Fig. 15a). The second one, about 0.4 m high and 0.25 m wide, affects clayey siltstone and red floodplain sandstone. This structure is filled with the same material and capped by undeformed lacustrine limestones. Its borders show microfaults and small synclinorium folds (Fig. 15b).

Interpretation. van Loon (1992, 2009) suggested that the formation of gravifossum is complex. Analysis of the gravifossums observed in the Outerbat syncline shows that the affected beds underwent liquefaction that first led to loading phenomena, such as load casts, and then faults would have accentuated the subsidence by giving it a micro-graben shape. The synclinal shape associated with hydroplastic folds could be caused by loading, as suggested by van Loon and Wiggers (1976). Like the load casts, these gravifossums are form by gravity in unstable clayey siltstones and fine sandstones at the time of deposition, and are associated with the reversed density gradients of Anketell et al. (1970).

4.3.9 Synsedimentary faults and fault-grading

Description. Numerous synsedimentary faults affect different beds in the Isli Formation. These faults are centimetre to metre-scale and affect laminae within the sandstone beds, or offset several beds (Fig. 16a–f). They are well preserved and mostly normal in terms of sense of motion, sometimes forming simple faults (Fig. 16c, d), grabens (Fig. 16b) and graded normal faults (Fig. 16a, e, f). They offset the sandstone, red clay siltstone and grey claystone layers. Their dips vary between 40° and 80°, and some are associated with other SSDS as load structures literally in the same beds.

Interpretation. Seilacher (1969) was the first to relate synsedimentary fault gradations to earthquakes. The beds containing these faults are also known as seismites. Deformation by these faults is interpreted as the result of low pore pressure in the still soft sediment (Maltman, 1994; Moretti & Sabato, 2007; Owen, 2003). The direction of the most of these faults is parallel to the direction of the major faults in the region, suggesting that these directional faults normally occur during sedimentation of the Isli Formation deposits. One of the determining criteria in distinguishing these

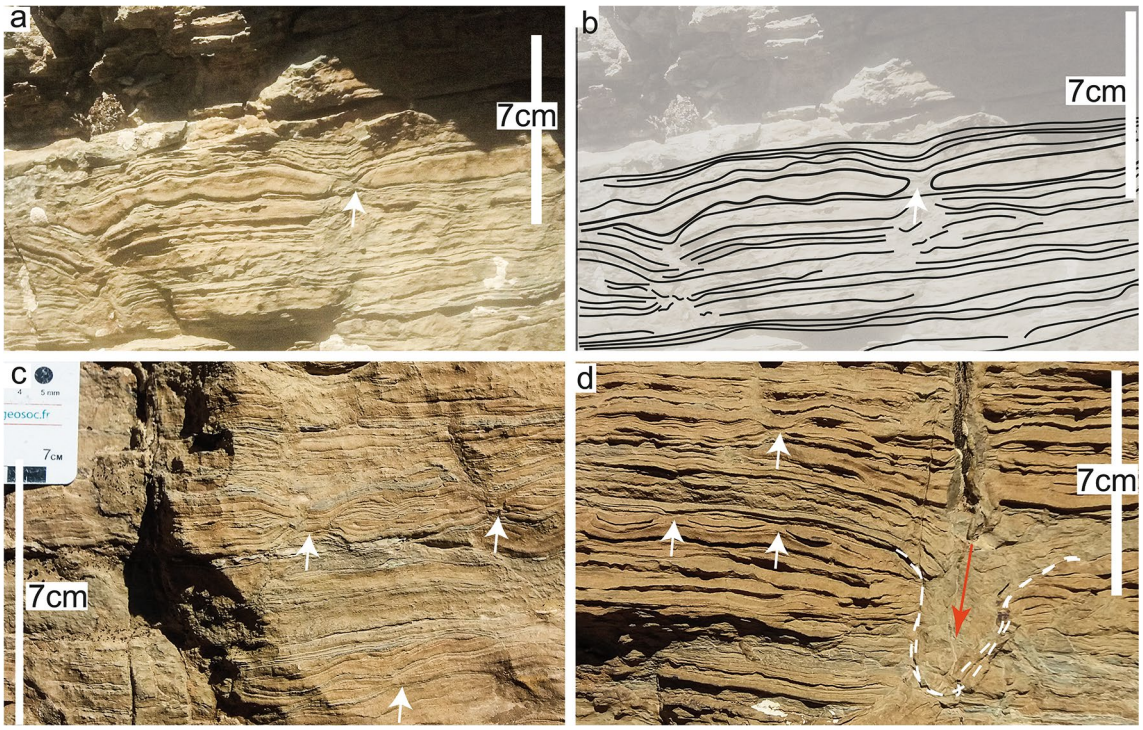

Fig. 14 Some photos of loop-bedding structures observed in the sedimentary beds of the Isli Formation. **a** Photograph. **b** Sketch of **a**. Loop bedding with disturbed, thickening and thinning lamina. **c** Loop bedding structures are visible in the same bed as **b**. **d** Loop bedding structures as stretched boudins (white arrows) associated with a Neptunian dyke (red arrow) in the same bed as **b** and **c**

faults from others of tectonic origin is their preservation by undeformed beds or laminations (Montenat et al., 2007). Beds containing similar synsedimentary faults have been described by several authors as soft-sediment deformation structures (e.g., Zanchi 1992; Bhattacharya & Bandyopadhyay, 1998; Koç-Taşgın et al., 2011; Kale et al., 2016; Ko et al., 2017; Koç-Taşgın & Diniz-Akarca, 2018; Chen et al., 2020; Hou et al., 2020; Neuwerth et al., 2006; Bhattacharya & Saha, 2020).

5 Discussion

After description, classification and the interpretation of driving forces and mechanisms of deformation of the SSDS, the identification of the triggering mechanism of the SSDS is the final and key step. In this paper, we followed the methodology of Owen and Moretti (2011).

The formation of SSDS is often due to liquefaction and fluidisation. This primary process occurs when a water-saturated sediment is subjected to sufficient stress or shaking, causing it to become liquid-like. Indeed, the mechanisms of deformation may be triggered by many different processes (Owen & Moretti, 2011; Owen et al., 2011b). The most common trigger is seismicity. An earthquake of magnitude of at least 5 is needed to cause liquefaction. In order to correctly assign the trigger for layers with SSDS, we must first exclude other possible triggers and then argue for the seismic trigger. The challenging task in the nomination of a deformed bed as a seismite is to exclude all other autogenic and allogenic possible triggers (Moretti & van Loon, 2014). Hereafter, in the following subsections, the discussion of many potential triggers begins. First, the exclusion of the control of facies on the formation of SSDS. Second, as the Isli Formation is rich in dinosaur and other tetrapod tracks and trackways, they can form SSDS-like features, especially those displayed in the section, known as dinoturbation, were excluded for SSDS reported in this work. Third, overloading, as known in the SSDS formation process, is also excluded based on sedimentological evidence. Fourth, as strong evidence of seismites, the basin's tectonic activity is provided, along with the geodynamic and seismic settings of the area during Isli Formation deposition. Finally, we discuss the possible seismic magnitudes that could produce seismites.

5.1 The facies-SSDS relationship

The studied formation extends over several tens of kilometres and the outcrop conditions are excellent, so that we could easily study most of the deformed beds over long distances. The soft-sediment deformation structures are well exposed in the different facies of the fluvio-lacustrine Isli

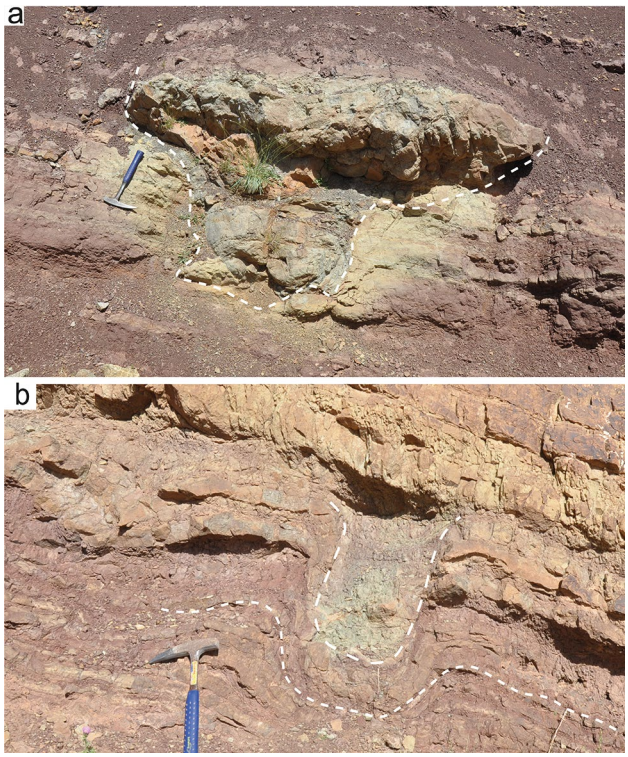

Fig. 15 Field photos of gravifossums. **a** Record of a fine sandstone gravifossum in clayey siltstone alternating with thin fine sandstone beds. **b** The gravifossum affects grey silty claystone and deforms an alternation of clayey siltstone and red fine sandstone beds at the bottom

Formation, dominated by fine grain sizes, favouring their formation (Lowe, 1976; van Loon, 2009). The sandstone beds of the FA3 facies association are the most deformed. This deformation disappears laterally in the fine floodplain deposits due to the change in grain size, density homogeneity and water saturation of the sediments at the time of the earthquakes (Alfaro et al., 2010; Civico et al., 2015; Ninfo et al., 2012). Indeed, we found that the floodplain deposits record only rare SSDS (synsedimentary faults, slumps and intrusions). We also noted that the size of SSDS such as load structures, depends on the thickness of the sandstone beds. SSDS which were formed in lacustrine carbonate beds did not continue laterally into other facies.

Although there is repetition of the same levels with identical facies characteristics over several hundred meters, only some beds recorded SSDS, suggesting that there may not be a direct relationship with specific facies types.

5.2 Exclusion of endogenic and exogenic triggers

The fluvio-lacustrine deposits of the Isli Formation were deposited in the distal zone of a large distributive fluvial system under a warm climate. In this context, certain triggers soft sediment deformation can be excluded, such as tsunamis, glacial loading and tidal shear. Furthermore, the deformed lake beds do not show any structures that would indicate storm waves such as hummocky cross stratification or the transport of sedimentary balls. The lack of evidence for a significant palaeoslope allows us to discard the action of gravitational instabilities. Furthermore, we found no evidence of high sedimentation rates in the facies of the studied formation, because the deformed beds and their underlying and overlying beds usually show fine laminations. Some structures, considered as SSDS (e.g., Ezquerro et al., 2015) and clearly related to endogenic triggers such as erosion surfaces, dissolution cavities, desiccation cracks, bioturbation and palaeosol beds with rhizoliths and nodules etc., are not considered in this work. Some triggers reported as causes of the formation of some types of soft-sediment deformation structures, such as dinosaur locomotion (dinoturbation) and overloading, are discussed below.

5.2.1 Dinoturbation

The Imilchil region can be qualified as a Type 3 megatracksite or a Zoological Ichnofaunal Province (ZIP) (sensu Lockley & Meyer, 2023) thanks to the exceptional richness of the Imilchil and Isli formations in dinosaur tracks and trackways, mainly of theropods and sauropods (Gierliński et al., 2009; 2017; Klein et al., 2018, 2023; Oukassou et al., 2019; Boutakiout et al., 2020; Masrour et al., 2020; Oussou et al., 2023). The locomotion of dinosaurs causes deformation of the still unlithified sediments, which produces structures that sometimes resemble those caused by other deformation mechanisms, notably simple load casts. The bioturbation structures left by dinosaurs (vertebrate bioturbation) are called dinoturbation (Carvalho et al., 2022; Christofoletti et al., 2021); these are not taken into account in this study. These structures are very limited in occurrence, with just one or two ichnosites in the study area. In addition, they show deformation of sediment partially liquefied. These features distinguish them from other SSDS such as load structures, folds and convolute lamination.

5.2.2 Overloading

We consider it unlikely that overloading is a trigger for deformation in the Isli Formation for the following reasons: (i) all facies in the SSDS beds are fine to very fine, well-graded and often finely laminated facies; (ii) the beds have kilometre-long extensions in a low-energy continental depositional environment; (iii) the thickest channel deposits are devoid of SSDS, and (iv) the deformed beds are framed by others which show no evidence of overloading. For all these reasons, overloading is unlikely to be the trigger for the SSDS studied here.

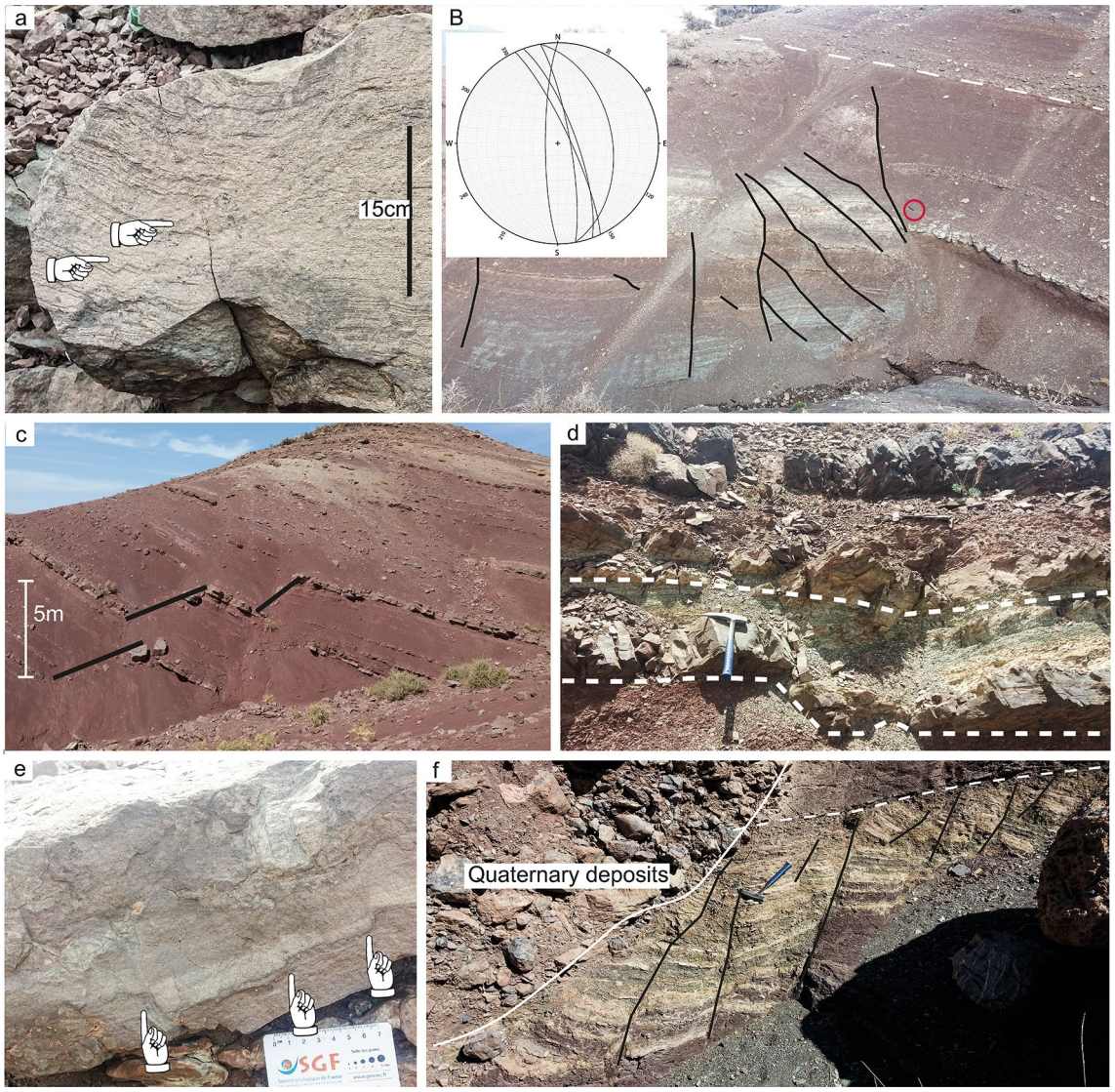

Fig. 16 Field photos showing some synsedimentary faults in the Isli Formation. **a** Normal microfaults (indicated by the hand symbol) affect horizontally laminated sandstone. **b** A bed affected by a gradation of synsedimentary horst and graben faults. **c** Superimposed normal faults well preserved by the upper beds affecting thin floodplain beds (N10; 50–75°W). **d** A synsedimentary normal fault marked by thickening of grey argillites. **e** Further micro-faults in laminations of a sandstone bed (N150; 50°W). **f** A gradation of synsedimentary normal faults (N65; 55°–80°NW)

5.3 Tectonic and seismic activity of the study area

The only remaining trigger for the SSDS, after exclusion of endogenic triggers such as dinoturbation or overloading is seismicity. The seismogenic faults could be those located along the ridges. The Isli Formation was deposited during the Bathonian-? Late Jurassic in an extensional setting with diapirism and the emplacement of magmatic intrusions. Salt tectonics produces several anticlinal ridges and synkinematic synclines (Joussiaume, 2016; Malaval et al., 2014; Michard et al., 2011; Moragas, 2017; Saura et al., 2014).

Along the edges of the boundary ridges, the formations form progressive unconformities (Ibouh, 1995, 2004; Ibouh & Chafiki, 2017). The Isli Formation is deposited in angular unconformities on the Tassent Formation in some places in the AAK syncline (Fadile, 2003), which is evidence of the tectonic activity of the ridges before and during the deposition of the Isli Formation. Synsedimentary normal faults and well-preserved tilted blocks in the various synclines (Fig. 16) also indicate that the formation was deposited under syntectonic conditions. Not far from the cores of the ridges, which consist mainly of CAMP basalts with intercalations of Triassic metamorphosed whitish red claystones, the studied formation shows that it was affected by the continuous upward movement of the ridges. This is reflected in the thickening of the beds towards the centre of

the basin (Fig. 2). These progressive unconformities are well exposed at the edges of the Plateau des Lacs and Outerbat synclines. Magmatic activity in the form of dolerite dykes, basaltic flows and gabbroic intrusions (Armando, 1999; Calvín et al., 2017) also indicate a geodynamical extensional setting during the deposition of the Isli Formation and prevailed throughout the Mesozoic Era in the central High Atlas (Warme, 1988; Frizon De Lamotte et al., 2009; Charrière et al., 2011; Torres-López et al., 2016; Calvín et al., 2017; Ibouh & Chafiki, 2017 Calvín et al., 2018a, 2018b; Ouaskou et al., 2021).

Researchers found that in most cases, to trigger liquefaction, earthquake epicentres (major faults) must be located within 40 km of the deformed beds (Galli, 2000; Moretti, 2000; Rodríguez-Pascua et al., 2000). In the study area, each syncline is surrounded by major faults (anticlinal ridges) active during the deposition of the formation in question, with a distance of less than 5 km from each seismite bed (Figs. 1b, 2). Indeed, the three synclines and their surrounding ridges are grouped together in an area whose diameter does not exceed 30 km.

The depositional environment corresponds to the distal zone of a large DFS interspersed with extensive lakes. It was formed as a result of tectonic subsidence caused by the reactivation of regional faults of the Palaeozoic basement. This depositional environment has played the role of broad lateral distribution of SSDS and is considered suitable to liquefaction (Galli, 2000 and references therein).

The lateral, sometimes kilometre-long, distribution and repetition of SSDS in different sedimentary beds are arguments in favour of a seismic origin of all beds with SSDS (Moretti & van Loon, 2014). The rise of anticlinal ridges may generate normal faults and neptunian dykes in adjacent synclines. Such normal faults form around diapiric structures (Alsop et al., 2000; Rowan et al., 2020). They may also be related to subsidence of the synclines during the extensive Jurassic tectonic phase in the area.

Jurassic seismicity in the study area is closely related to the major normal faults that were active during the Isli Formation deposition. These NE-trending Palaeozoic basement faults have moved in an extensional setting. It is important to note that these faults have considerable dimensions, extending over tens of kilometres (Fig. 17). With regard to the depth of these faults, they penetrate to over 5000 m, which is the total thickness of the Jurassic cover in the study area. These seismogenic faults caused seismic shaking that led to an increase in pore-fluid pressure in the water-saturated sediments.

5.4 Earthquake magnitudes

The estimation of the magnitude of the earthquakes responsible for the formation of SSDS is controversial. Guiraud and Plaziat (1993) and Rodríguez-Pascua et al. (2000) have proposed a scheme to distinguish magnitudes according to the type of SSDS. Obermeier (1996) also estimated magnitudes based on the size of the SSDS. Galli (2000) showed that there is a link between the distance from earthquake source and the magnitude of the formation of liquefaction-induced structures. However, Moretti and Sabato (2007) and Alfaro et al. (2010) have criticised these magnitude estimates. It is known that, in order to cause liquefaction, an earthquake magnitude of at least 5 is needed. The SSDS that formed without liquefaction, such as loop bedding structures, may require smaller magnitude earthquakes (Berra & Felletti, 2011; Rodríguez-Pascua et al., 2000).

In our study area, the three synclinal "mini-basins" studied are delimited by four anticlinal ridges. These major Atlasic faults inherited from the Hercyinian orogeny are still active (Medina & Cherkaoui, 2021). Galli (2000) proposed a diameter of less than 40 km from the epicentre for a magnitude 6 earthquake to generate SSDS. It is very difficult to link an SSDS bed to a specific fault. The exposure of beds in synclines is mostly parallel to the main faults in the area (Fig. 1b), making it difficult to prove the zonation of SSDS (Moretti & van Loon, 2014; Owen & Moretti, 2011) in the deformed beds.

6 Summary and conclusion

This paper presents the first sedimentological study of the Jurassic red beds in the axis of the Atlas system, and focuses on the fluvio-lacustrine sediments of the Bathonian-? Upper Jurassic Isli Formation. The depositional environment of the Isli Formation corresponds to the distal zone of a large Distributary Fluvial System (DFS) with large lacustrine areas. This palaeoenvironment formed following eastward retreat of the Tethyian Sea from the entire Atlas system.

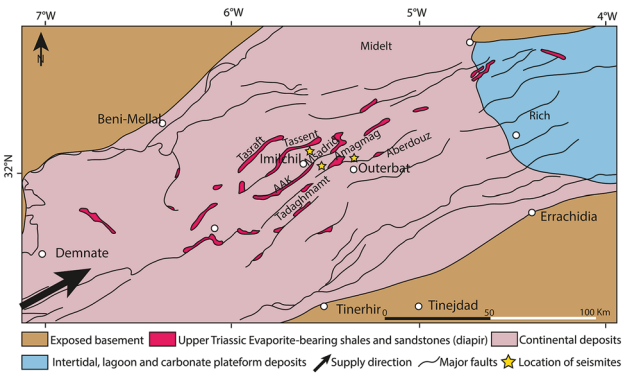

Fig. 17 Regional palaeogeographic map (Bathonian-Callovian interval) showing major faults in the study area (after Moragas, 2017)

Table 2 Driving forces, deformation mechanisms, and trigger mechanisms of the different soft-sediment deformation structures observed in the Isli formation

Soft-sediment deformation structures	Description	Driving force	Mechanism of deformation	Trigger mechanisms
Neptunian dykes	Open and widening upward metre-scale cracks filled by sandstones descending in the host layers and causing brecciation in the case of sills	Extension stress	brittle deformation	Extensional tectonics or earthquake
Load casts	Small discontinuous downward displacement of sedimentary masses in the sediment of the liquefied matrix	Reversed density gradients	Liquefaction	Earthquake
Attached and detached pseudonodules	Non-continuous vertical displacement of sandstone masses still attached to and detached from the source layer	Reversed density gradients	Liquefaction and fluidisation	Earthquake
Ball and pillow structures	Sandstone balls completely cut out of the source layer and rooted in the sediment with different composition of the matrix	Reversed density gradients	Liquefaction and fluidisation	Earthquake
Flames structures	Decimetre-scale upward displacement of silty clays and silts in the form of diapirs associated with load casts	Reversed density gradients	Liquefaction and fluidisation	Earthquake
Isolated plastic intrusions	Decimetre-scale upward and horizontal displacement of siltstones and silty clays	Reversed density gradients	Liquefaction and fluidisation	Earthquake
Slump folds	Several centimeter- to meter-scale slump folds. Some of these folds are nearly recumbent and show short and long flanks, while others form laterally continuous synclinal and anticlinal disharmonic folds	Gravitational force and local compressional stress	Liquefaction and hydroplasticity	Earthquakes and slumping
Convolute lamination structures	Centimetre-scale deformation in anticlinal and synclinal folding of the laminae within the fine sediment beds (fine sandstone and siltstone)	Reversed bulk-density gradient	Liquefaction	Earthquake
Cusp structures	Millimetre to centimetre upward displacement of the sediment within horizontally laminated sandstone and limestone beds	Vertical shear stress	Fluidisation	Earthquake
Injection dyke	A metre-scale, upwardly thinning, dyke formed by carbonate sandstones	Fluid overpressure and hydrofracturing	Liquefaction and fluidisation	Earthquake and/or rapid loading

Table 2 (continued)

Soft-sediment deformation structures	Description	Driving force	Mechanism of deformation	Trigger mechanisms
Loop bedding structures	Centimetre-scale deformation of laminae groups in limestones with lateral thinning and thickening	Tensional stress of the sediments (local stress)	Hydroplastic	Earthquake
Gravifossum structures	Decimetre-scale displacement downwards in the same sediment and formation of a depression dominated by graben faults and synclinal folds (plastic deformation)	Reversed density gradients	Plastic deformation/fluidisation/liquefaction	Loading/earthquake
Synsedimentary faults	Shifting movements of a few sedimentary beds and sometimes of a few laminae within a bed	Extensive stresses	Quasi-brittle deformation	Earthquake and tectonic

Soft sediment deformation is very common in the Isli Formation. Several types of soft-sediment deformation structures have been described: neptunian dykes, slumps, load structures, slump folds, convolute lamination structures, water-escape structures (cusps and injection dyke), loop beddings and gravifossums. The analysis of these soft-sediment deformation structures show that they have been deformed by liquefaction and fluidisation.

Several criteria for seismite recognition have been verified and confirmed, namely: (i) all deformed beds are separated by undeformed ones, (ii) the beds are continuous over long distances, (iii) there is evidence of an active tectonic regime during the deposition of the beds, (iv) similarity of the observed SSDS with current earthquake-induced SSDS, and (v) vertical repetition of certain beds of the same deformation style.

The liquefaction and fluidisation that led to the formation of the SSDS in the Jurassic Red Beds of the Atlas Belt axis are, with reference to the current data, the result of earthquakes (Table 2).

The frequency and distribution of seismite beds in the three studied synclines of the High Atlas allow us to conclude that several faults were active during sedimentation of the Isli Formation Red Beds (lower Bathonian-? Upper Jurassic). This tectonic activity could be related to salt tectonics along the ridges.

Acknowledgements All of the authors express their sincere gratitude to the Editor-in-Chief, Prof. Javier Martín-Chivelet, and the reviewer, Prof. Pedro Alfaro, as well as an anonymous reviewer, for their valuable constructive comments and suggestions during the peer-review process. We would also like to extend our thanks to Susannah C.R. Maidment from the Natural History Museum of London (NHML) and Said Oussou from Moulay Ismail University (Morocco) for their contributions in improving the manuscript's English.

Data availability No data was used for this paper.

Declarations

Conflict of interest The authors declare that they have no known competing financial interests or personal relationships that that are relevant to the content of this article.

References

Alencar, M. L., Correia Filho, O. J., de Miranda, T. S., Barbosa, J. A., Celestino, M. A. L., Ramos, G. M. S., Araújo, A. F., Neumann, V. H., Topan, J. G., & Roemers-Oliveira, E. (2021). Soft-sediment deformation structures in Aptian lacustrine laminites: Evidence of post-rift paleoseismicity in the Araripe basin, NE Brazil. *Journal of South American Earth Sciences, 105*, 102955. https://doi.org/10.1016/j.jsames.2020.102955

Alfaro, P., Moretti, M., & Owen, G. (Eds), (2016). The environmental significance of soft sediment deformation. *Sedimentary Geology*, 344.

Alfaro, P., Gibert, L., Moretti, M., García-Tortosa, F. J., Sanz de Galdeano, C., Galindo-Zaldívar, J., & López-Garrido, Á. C. (2010). The significance of giant seismites in the Plio-Pleistocene Baza palaeo-lake (S Spain). *Terra Nova, 22*(3), 172–179. https://doi.org/10.1111/j.1365-3121.2010.00930.x

Alfaro, P., Moretti, M., & Soria, J. M. (1997). Soft-sediment deformation structures induced by earthquakes (seismites) in Pliocene lacustrine deposits (Guadix-Baza Basin. Central Betic cordillera). *Eclogae Geologicae Helvetiae, 90*(3), 531–540.

Ali, U., & Ali, S. A. (2018). Seismically induced soft-sediment deformation structures in an active seismogenic setting: the Plio-Pleistocene Karewa deposits, Kashmir Basin (NW Himalaya). *Journal of Structural Geology, 115*, 28–46. https://doi.org/10.1016/j.jsg.2018.07.005

Allen, J. R. (1977). The possible mechanics of convolute lamination in graded sand beds. *Journal of the Geological Society, 134*(1), 19–31. https://doi.org/10.1144/gsjgs.134.1.0019

Alonso-Zarza, A.M., & Wright, V.P. (2010). Calcretes. In A.M. Alonso-Zarza, & L.H. Tanner (Eds.), Continental Carbonates. Facies, Environments and Processes. *Developments in Sedimentology, 61* (pp. 225–267) Elsevier. https://doi.org/10.1016/S0070-4571(09)06105-6

Alsop, G. I., Brown, J. P., Davison, I., & Gibling, M. R. (2000). The geometry of drag zones adjacent to salt diapirs. *Journal of the Geological Society, 157*(5), 1019–1029. https://doi.org/10.1144/jgs.157.5.1019

Alsop, G. I., & Marco, S. (2013). Seismogenic slump folds formed by gravity-driven tectonics down a negligible subaqueous slope. *Tectonophysics, 605*, 48–69. https://doi.org/10.1016/j.tecto.2013.04.004

Alsop, G. I., Weinberger, R., Marco, S., & Levi, T. (2019). Identifying soft-sediment deformation in rocks. *Journal of Structural Geology, 125*, 248–255. https://doi.org/10.1016/j.jsg.2017.09.001

Alsop, G. I., Weinberger, R., Marco, S., & Levi, T. (2020). Folding during soft-sediment deformation. *Geological Society, London, Special Publications, 487*(1), 81–104. https://doi.org/10.1144/SP487.1

Anketell, J. M., Cegła, J., & Dżułyński, S. (1970). On the deformational structures in systems with reversed density gradients. In *Annales Societatis Geologorum Poloniae* (Vol. 40, No. 1, pp. 3–30).

Armando, G. (1999). Intracontinental alkaline magmatism: Geology, petrography, mineralogy and geochemistry of the Jebel Hayim Massif (central High Atlas-Morocco). *Mémoires De Géologie De L'université De Lausanne, 31*, 106.

Ayarza, P., Alvarez-Lobato, F., Teixell, A., Arboleya, M. L., Teson, E., Julivert, M., & Charroud, M. (2005). Crustal structure under the central High Atlas Mountains (Morocco) from geological and gravity data. *Tectonophysics, 400*(1–4), 67–84. https://doi.org/10.1016/j.tecto.2005.02.009

Azennoud, K., Baali, A., El Asmi, H., Brahim, Y. A., Hakam, O., Hayati, A., & El Kamel, T. (2022). Soft-sediment deformation structures recognised in a reverse-drag associated with normal faulting (Lake Ifrah, Northwest Africa): Palaeoseismic assessment and neotectonic implications. *Sedimentary Geology, 441*, 106264. https://doi.org/10.1016/j.sedgeo.2022.106264

Bachmann, G. H., & Aref, M. A. (2005). A seismite in Triassic gypsum deposits (Grabfeld Formation, Ladinian), southwestern Germany. *Sedimentary Geology, 180*(1–2), 75–89. https://doi.org/10.1016/j.sedgeo.2005.04.006

Barbero, L., Teixell, A., Arboleya, M. L., Río, P. D., Reiners, P. W., & Bougadir, B. (2007). Jurassic-to-present thermal history of the central High Atlas (Morocco) assessed by low-temperature thermochronology. *Terra Nova, 19*(1), 58–64. https://doi.org/10.1111/j.1365-3121.2006.00715.x

Benabbou, M., Alaoui, B. L., & Baali, A. (2018). Structures de déformation hydroplastique d'origine sismique dans les dépôts lacustres du Pléistocène supérieur de dayet Iffer (Moyen Atlas, Maroc). *Quaternaire, 29*(4), 295–310. https://doi.org/10.4000/quaternaire.10495

Berger, A., & Herwegh, M. (2019). Cockade structures as a paleo-earthquake proxy in upper crustal hydrothermal systems. *Scientific Reports, 9*(1), 1–9. https://doi.org/10.1038/s41598-019-45488-2

Berra, F., & Felletti, F. (2011). Syndepositional tectonics recorded by soft-sediment deformation and liquefaction structures (continental Lower Permian sediments, Southern Alps, Northern Italy): stratigraphic significance. *Sedimentary Geology, 235*(3–4), 249–263. https://doi.org/10.1016/j.sedgeo.2010.08.006

Bhattacharya, B., & Saha, A. (2020). Large soft-sediment deformation structures (SSDS) in the Permian Barren Measures Formation, Pranhita-Godavari Valley, India: Potential link to syn-rift palaeoearthquake events. *Journal of Palaeogeography, 9*(1), 1–18. https://doi.org/10.1186/s42501-020-00063-z

Bhattacharya, H. N., & Bandyopadhyay, S. (1998). Seismites in a Proterozoic tidal succession, Singhbhum, Bihar, India. *Sedimentary Geology, 119*(3–4), 239–252. https://doi.org/10.1016/S0037-0738(98)00051-7

Boutakiout, M., Masrour, M., & Pérez-Lorente, F. (2020). New sauropod morphotype definition in the oriental sec tion 0F Imilchil megatracksite, high atlas (Morocco). *Journal of African Earth Sciences, 161*, 103664. https://doi.org/10.1016/j.jafrearsci.2019.103664

Calvín, P., Casas-Sainz, A. M., Villalaín, J. J., & Moussaid, B. (2018b). Extensional vs. compressional deformation in the Central High Atlas salt province: a paleomagnetic approach. *Tectonophysics, 734*, 130–147. https://doi.org/10.1016/j.tecto.2018.04.007

Calvín, P., Ruiz-Martínez, V. C., Villalaín, J. J., Casas-Sainz, A. M., & Moussaid, B. (2017). Emplacement and deformation of Mesozoic gabbros of the High Atlas (Morocco): Paleomagnetism and magnetic fabrics. *Tectonics, 36*(12), 3012–3037. https://doi.org/10.1002/2017TC004578

Calvín, P., Villalaín, J. J., & Casas-Sainz, A. M. (2018a). Anisotropic magnetite growth in remagnetized limestones: Tectonic constraints and implications for basin history. *Geology, 46*(9), 751–754. https://doi.org/10.1130/G45158.1

Calvo, J. P., Rodríguez-Pascua, M., Martin-Velazquez, S., Jimenez, S., & Vicente, G. D. (1998). Microdeformation of lacustrine laminite sequences from Late Miocene formations of SE Spain: An interpretation of loop bedding. *Sedimentology, 45*(2), 279–292. https://doi.org/10.1046/j.1365-3091.1998.00145.x

Carvalho, I. S., Cunha, P. P., & Figueiredo, S. M. (2022). Dinoturbation in Upper Jurassic siliciclastic levels at Cabo Mondego (Lusitanian Basin, Portugal): Evidences in a fluvial-dominated deltaic succession. *Palaeoworld, 31*(3), 455–477. https://doi.org/10.1016/j.palwor.2021.09.001

Ceniceros, J. M., Farlow, J. O., Masrour, M., Extremiana, J. I., Boutakiout, M., & Pérez-Lorente, F. (2022). Demographic interpretation of colossal theropod footprints discoveries from Imilchil (Mid-Jurassic, Central High Atlas, Morocco). *Journal of African Earth Sciences*. https://doi.org/10.1016/j.jafrearsci.2022.104595

Charrière, A., Ibouh, H., & Haddoumi, H. (2011). Circuit C7, Le Haut Atlas central de Beni Mellal à Imilchil. In A. Michard, O. Saddiqi, A. Chalouan, & A. Mouttaqi (Eds.), *Nouveaux guides géologiques et miniers du Maroc* (pp. 109–164). *Notes et Mémoires du Service Géologique du Maroc, 559*.

Charrière, A., & Haddoumi, H. (2017). Dater les couches rouges continentales pour définir la géodynamique atlasique. *Géologues, 194*, 29–32.

Charrière, A., Haddoumi, H., Mojon, P. O., Ferrière, J., Cuche, D., & Zili, L. (2009). Mise en évidence par charophytes et ostracodes de l'âge Paléocène des dépôts discordants sur les rides anticlinales de la région d'Imilchil (Haut Atlas, Maroc):

Conséquences paléogéographiques et structurales. *Comptes Rendus Palevol, 8*(1), 9–19. https://doi.org/10.1016/j.crpv.2008.11.006

Chen, A., Zhong, Y., Ogg, J. G., van Loon, A. T., Chen, H., Yang, S., Liu, L., & Xu, S. (2020). Traces of the Triassic collision between the North and South China blocks in the form of seismites and other event layers. *Journal of Geodynamics, 136*, 101720. https://doi.org/10.1016/j.jog.2020.101720

Christofoletti, B., Peixoto, B. C., Warren, L. V., Inglez, L., Fernandes, M. A., Alessandretti, L., Perinotto, A. J. A., & Assine, M. L. (2021). Dinos among the dunes: Dinoturbation in the Pirambóia Formation (Paraná Basin), São Paulo State and comments on cross-section tracks. *Journal of South American Earth Sciences, 109*, 103252. https://doi.org/10.1016/j.jsames.2021.103252

Civico, R., Brunori, C. A., De Martini, P. M., Pucci, S., Cinti, F. R., & Pantosti, D. (2015). Liquefaction susceptibility assessment in fluvial plains using airborne lidar: the case of the 2012 Emilia earthquake sequence area (Italy). *Natural Hazards and Earth System Sciences, 15*(11), 2473–2483. https://doi.org/10.5194/nhess-15-2473-2015

Collinson, J. (2005). Post-depositional sedimentary structures. In R. C. Selley, L. R. M. Cocks, & I. R. Plimer (Eds.), *Encyclopedia of geology* (pp. 602–611). Elsevier.

Collinson, J. D., & Mountney, N. P. (2019). *Sedimentary structures* (4th ed.). Edinburgh: Dunedin Academic Press.

Dasgupta, P. (2008). Experimental decipherment of the soft-sediment deformation observed in the upper part of the Talchir Formation (Lower Permian), Jharia Basin, India. *Sedimentary Geology, 205*(3–4), 100–110. https://doi.org/10.1016/j.sedgeo.2008.01.006

Davies, N. S., Turner, P., & Sansom, I. J. (2005). Soft-sediment deformation structures in the Late Silurian Stubdal Formation: The result of seismic triggering. *Norwegian Journal of Geology, 85*(3), 233–244.

Dechen, S., & Aiping, S. (2012). Typical earthquake-induced soft-sediment deformation structures in the Mesoproterozoic Wumishan Formation, Yongding River Valley, Beijing, China and interpreted earthquake frequency. *Journal of Palaeogeography, 1*(1), 71–89. https://doi.org/10.3724/SP.J.1261.2012.00007

Dooley, T. P., & Hudec, M. R. (2020). Extension and inversion of salt-bearing rift systems. *Solid Earth, 11*(4), 1187–1204. https://doi.org/10.5194/se-11-1187-2020

El Taki, H., & Pratt, B. R. (2012). Syndepositional tectonic activity in an epicontinental basin revealed by deformation of subaqueous carbonate laminites and evaporites: seismites in Red River strata (Upper Ordovician) of southern Saskatchewan, Canada. *Bulletin of Canadian Petroleum Geology, 60*(1), 37–58. https://doi.org/10.2113/gscpgbull.60.1.37

Elmi S. (1999). Cartes paleogéographiques, in (Anonyme) Maroc, Mémoire de la Terre, *Ed. Mus. Nat. Hist. Nat. Paris,* 2 pl. h-t.

Escosa, F. O., Leprêtre, R., Spina, V., Gimeno-Vives, O., Kergaravat, C., Mohn, G., & de Lamotte, D. F. (2021). Polyphased mesozoic rifting from the Atlas to the north-west Africa paleomargin. *Earth-Science Reviews, 220*, 103732. https://doi.org/10.1016/j.earscirev.2021.103732

Essaifi, A., & Zayane, R. (2018). Petrogenesis and origin of the Upper Jurassic-Lower Cretaceous magmatism in Central High Atlas (Morocco): major, trace element and isotopic (Sr-Nd) constraints. *Journal of African Earth Sciences, 137*, 229–245. https://doi.org/10.1016/j.jafrearsci.2017.10.002

Ettaki, M., Ibouh, H., Chellaï, E. H., & Milhi, A. (2007). Les structures" diapiriques" liasiques du Haut-Atlas central, Maroc: exemple de la ride d'Ikerzi. *Africa Geoscience Review, 14*(1–2), 79.

Ettensohn, F. R., Rast, N., & Brett, C. E. (Eds.). (2002). *Ancient seismites*. *Geological Society of America, 359*. https://doi.org/10.1130/SPE359

Ezquerro, L., Moretti, M., Liesa, C. L., Luzón, A., & Simón, J. L. (2015). Seismites from a well core of palustrine deposits as a tool for reconstructing the palaeoseismic history of a fault. *Tectonophysics, 655*, 191–205. https://doi.org/10.1016/j.tecto.2015.05.025

Fadile, A. (2003). Carte géologique du Maroc au 1/100 000, feuille d'Imilchil. *Notes et Mémoires du Service géologique du Maroc*, *397*.

Fekkak, A., Ouanaimi, H., Michard, A., Soulaimani, A., Ettachfini, E. M., Berrada, I., El Arabi, H., Lagnaoui, A., & Saddiqi, O. (2018). Thick-skinned tectonics in a Late Cretaceous-Neogene intracontinental belt (High Atlas Mountains, Morocco): The flat-ramp fault control on basement shortening and cover folding. *Journal of African Earth Sciences, 140*, 169–188. https://doi.org/10.1016/j.jafrearsci.2018.01.008

Festa, A., Dilek, Y., Gawlick, H.-J., Missoni, S., (Eds.). (2014). Mass-transport deposits, olistostromes and soft-sediment deformation in modern and ancient continental margins, and associated natural hazards [Special issue]. *Marine Geology, 356.*

Flügel, E. (2010). *Microfacies of carbonate rocks: Analysis, interpretation and application*. Springer.

Frizon de Lamotte, D., Zizi, M., Missenard, Y., Hafid, M., El Azzouzi, M., Maury, R.C., Charrière, A., Taki, Z., Benammi, M., & Michard, A. (2008). The Atlas system. In A. Michard, O. Saddiqi, A. Chalouan, & D. Frizon de Lamotte (Eds.), *The Geology of Morocco: Structure, stratigraphy, and Tectonics of the Africa-Atlantic-Mediterranean Triple Junction* (pp. 133–202). *Lecture Notes in Earth Sciences, 116*. https://doi.org/10.1007/978-3-540-77076-3_4

Frizon de Lamotte, D., Leturmy, P., Missenard, Y., Khomsi, S., Ruiz, G., Saddiqi, O., Guillocheau, F., & Michard, A. (2009). Mesozoic and Cenozoic vertical movements in the Atlas system (Algeria, Morocco, Tunisia): an overview. *Tectonophysics, 475*(1), 9–28. https://doi.org/10.1016/j.tecto.2008.10.024

Fullea, J., Fernàndez, M., Afonso, J. C., Vergés, J., & Zeyen, H. (2010). The structure and evolution of the lithosphere–asthenosphere boundary beneath the Atlantic-Mediterranean Transition Region. *Lithos, 120*(1–2), 74–95. https://doi.org/10.1016/j.lithos.2010.03.003

Galli, P. (2000). New empirical relationships between magnitude and distance for liquefaction. *Tectonophysics, 324*(3), 169–187. https://doi.org/10.1016/S0040-1951(00)00118-9

García-Tortosa, F. J., Alfaro, P., Gibert, L., & Scott, G. (2011). Seismically induced slump on an extremely gentle slope (< 1) of the Pleistocene Tecopa paleolake (California). *Geology, 39*(11), 1055–1058. https://doi.org/10.1130/G32218.1

Ghosh, S. K., Pandey, A. K., Pandey, P., Ray, Y., & Sinha, S. (2012). Soft-sediment deformation structures from the Paleoproterozoic Damtha Group of Garhwal Lesser Himalaya, India. *Sedimentary Geology, 261–262*, 76–89. https://doi.org/10.1016/j.sedgeo.2012.03.006

Gierliński, G. G., Menducki, P., Janiszewska, K., Wicik, I., & Boczarowski, A. (2009). A preliminary report on dinosaur track assemblages from the Middle Jurassic of the Imilchil area, Morocco. *Geological Quarterly, 53*(4), 477–482.

Granado, P., Ruh, J. B., Santolaria, P., Strauss, P., & Muñoz, J. A. (2021). Stretching and contraction of extensional basins with pre-rift salt: A numerical modeling approach. *Frontiers in Earth Science, 9*, 648937. https://doi.org/10.3389/feart.2021.648937

Guiraud, M., & Plaziat, J. C. (1993). Seismites in the fluviatile Bima sandstones: Identification of paleoseisms and discussion of their magnitudes in a Cretaceous synsedimentary strike-slip basin (Upper Benue, Nigeria). *Tectonophysics, 225*(4), 493–522. https://doi.org/10.1016/0040-1951(93)90312-8

Harris, C., Murton, J., & Davies, M. C. (2000). Soft-sediment deformation during thawing of ice-rich frozen soils: Results of scaled

centrifuge modelling experiments. *Sedimentology, 47*(3), 687–700. https://doi.org/10.1046/j.1365-3091.2000.00322.x

Hartley, A. J., Weissmann, G. S., Nichols, G. J., & Warwick, G. L. (2010). Large distributive fluvial systems: Characteristics, distribution, and controls on development. *Journal of Sedimentary Research, 80*(2), 167–183. https://doi.org/10.2110/jsr.2010.016

Hou, Z., Chen, S., Zhang, S., & Yang, H. (2020). Sedimentary deformation features as evidence for paleoseismic events in the middle Eocene in the Dongying Depression of the southern Bohai Bay Basin, eastern China. *Canadian Journal of Earth Sciences, 57*(8), 954–970. https://doi.org/10.1139/cjes-2019-016

Ibouh, H. (1995). Tectonique en décrochement et intrusions magmatiques au Jurassique; tectogenèse polyphasée des rides jurassiques d'Imilchil (Haut Atlas central, Maroc). *Ph.D Thesis.* Cadi Ayyad University, Marrakech, Morocco.

Ibouh, H. (2004). Du rift avorté au bassin sur décrochement, contrôles tectonique et sédimentaire pendant le Jurassique (Haut Atlas central, Maroc). *Ph.D Thesis*. Cadi Ayyad University, Marrakech, Morocco.

Ibouh, H., & Chafiki, D. (2017). La tectonique de l'Atlas: âge et modalités. *Géologues., 194*, 24–28.

Ibouh, H., Michard, A., Charriere, A., Benkaddour, A., & Rhoujjati, A. (2014). Tectonic–karstic origin of the alleged "impact crater" of Lake Isli (Imilchil district, High Atlas, Morocco). *Comptes Rendus Geoscience, 346*(3–4), 82–89. https://doi.org/10.1016/j.crte.2014.03.005

Jones, M. E., & Preston, R. M. F. (Eds.). (1987). *Deformation of sediments and sedimentary rocks* (p. 29). Geological Society. Special Publication.

Joussiaume, R., (2016). Les relations entre diapirisme et sédimentation: Exemple du Jurassique moyen de la région d'Imilchil, Haut-Atlas central, Maroc. *Ph.D. Thesis*. Bordeaux Montaigne University, Bordeaux, France.

Kale, M. G., Pundalik, A. S., Duraiswami, R. A., & Karmalkar, N. R. (2016). Soft sediment deformation structures from Khari River section of Rudramata member, Jhuran Formation, Kutch: A testimony of Jurassic seismites. *Journal of the Geological Society of India, 87*(2), 194–204. https://doi.org/10.1007/s12594-016-0387-8

Klausen, T. G., Ryseth, A. E., Helland-Hansen, W., Gawthorpe, R., & Laursen, I. (2014). Spatial and temporal changes in geometries of fluvial channel bodies from the Triassic Snadd Formation of offshore Norway. *Journal of Sedimentary Research, 84*(7), 567–585. https://doi.org/10.2110/jsr.2014.47

Klein, H., Gierliński, G. D., Oukassou, M., Saber, H., Lallensack, J. N., Lagnaoui, A., Hminna, A., & Charrière, A. (2023). Theropod and ornithischian dinosaur track assemblages from Middle to? Late Jurassic deposits of the Central High Atlas, Morocco. *Historical Biology, 35*(3), 320–346. https://doi.org/10.1080/08912963.2022.2042808

Klein, H., Lagnaoui, A., Gierliński, G. D., Saber, H., Lallensack, J. N., Oukassou, M., & Charrière, A. (2018). Crocodylomorph, turtle and mammal tracks in dinosaur-dominated Middle–? Upper Jurassic and mid-Cretaceous ichnoassemblages of Morocco. *Palaeogeography, Palaeoclimatology, Palaeoecology, 498*, 39–52. https://doi.org/10.1016/j.palaeo.2018.02.028

Knaust, D. (2002). Pinch-and-swell structures at the Middle/Upper Muschelkalk boundary (Triassic): Evidence of earthquake effects (seismites) in the Germanic Basin. *International Journal of Earth Sciences, 91*(2), 291–303. https://doi.org/10.1007/s005310100225

Ko, K., Kim, S. W., Lee, H. J., Hwang, I. G., Kim, B. C., Kee, W. S., Kim, Y. S., & Gihm, Y. S. (2017). Soft sediment deformation structures in a lacustrine sedimentary succession induced by volcano-tectonic activities: An example from the Cretaceous Beolgeumri Formation, Wido Volcanics, Korea. *Sedimentary Geology, 358*, 197–209. https://doi.org/10.1016/j.sedgeo.2017.07.008

Koç-Taşgın, C. (2011). Seismically-generated hydroplastic deformation structures in the Late Miocene lacustrine deposits of the Malatya Basin, eastern Turkey. *Sedimentary Geology, 235*(3–4), 264–276. https://doi.org/10.1016/j.sedgeo.2010.09.015

Koç-Taşgın, C. (2017). Soft-sediment deformation related to syntectonic intraformational unconformity in the early Palaeocene alluvial-fan deposits of Kuşçular Formation in the Elazığ sector of Tauride foreland, eastern Turkey. *Journal of African Earth Sciences, 134*, 665–677. https://doi.org/10.1016/j.jafrearsci.2017.07.030

Koç-Taşgın, C., & Diniz-Akarca, C. (2018). Soft-sediment deformation structures related to tectonomagmatic activity: A case study from the borate-bearing lacustrine deposits of early Miocene Bigadiç Basin, NW Turkey. *Sedimentary Geology, 373*, 32–47. https://doi.org/10.1016/j.sedgeo.2018.05.012

Koç-Taşgın, C. K., & Türkmen, İ. (2009). Analysis of soft-sediment deformation structures in Neogene fluvio-lacustrine deposits of Çaybağı Formation, Eastern Turkey. *Sedimentary Geology, 218*(1–4), 16–30. https://doi.org/10.1016/j.sedgeo.2009.04.009

Kuenen, P. H. (1958). Experiments in Geology. *Transactions of the Geological Society of Glasgow, 23*, 1–28. https://doi.org/10.1144/transglas.23.centenary.1

Kundu, A., Eriksson, P. G., & Matin, A. (2015). Soft-sediment deformation structures in the sub-Himalayan Middle Siwalik Subgroup, Lish River section, India. *Episodes Journal of International Geoscience, 38*(3), 197–207. https://doi.org/10.18814/epiiugs/2015/v38i3/006

Lanari, R., Faccenna, C., Natali, C., ŞengülUluocak, E., Fellin, M. G., Becker, T. W., Göğüş, O. H., Youbi, N., Clementucci, R., & Conticelli, S. (2023). The Atlas of Morocco: A Plume-Assisted Orogeny. *Geochemistry, Geophysics, Geosystems, 24*(6), e2022GC010843. https://doi.org/10.1029/2022GC010843

Laville, E., & Piqué, A. (1992). Jurassic penetrative deformation and Cenozoic uplift in the central High Atlas (Morocco): A tectonic model. Structural and orogenic inversions. *Geologische Rundschau, 81*(1), 157–170. https://doi.org/10.1007/BF01764546

Liesa, C. L., Rodríguez-López, J. P., Ezquerro, L., Alfaro, P., Rodríguez-Pascua, M. Á., Lafuente, P., Arlegui, L., & Simón, J. L. (2016). Facies control on seismites in an alluvial–aeolian system: The Pliocene dunefield of the Teruel half-graben basin (eastern Spain). *Sedimentary Geology, 344*, 237–252. https://doi.org/10.1016/j.sedgeo.2016.05.009

Lockley, M. G., & Meyer, C. A. (2023). The megatracksite phenomenon: Implications for tetrapod palaeobiology across terrestrial-shallow-marine transitional zones. *Geological Society, London, Special Publications, 522*(1), 285–324. https://doi.org/10.1144/SP522-2021-164

Lowe, D. R. (1975). Water escape structures in coarse-grained sediments. *Sedimentology, 22*(2), 157–204. https://doi.org/10.1111/j.1365-3091.1975.tb00290.x

Lowe, D. R. (1976). Grain flow and grain flow deposits. *Journal of Sedimentary Research, 46*(1), 188–199. https://doi.org/10.1306/212F6EF1-2B24-11D7-8648000102C1865D

Lunina, O. V., & Gladkov, A. S. (2016). Soft-sediment deformation structures induced by strong earthquakes in southern Siberia and their paleoseismic significance. *Sedimentary Geology, 344*, 5–19. https://doi.org/10.1016/j.sedgeo.2016.02.014

Malaval, M., Joussiaume, R., Razin, P., Grélaud, C., Messager, G., Martín-Martín, J.D., Saura, E., Moragas, M., Vergés, J., & Hunt, D. (2014). Characterization of Syn-Diapiric Jurassic Sedimentation in the Imilchil Area, Central High Atlas, Morocco. *19th International Sedimentological Congress, Geneva, Switzerland, International Association of Sedimentologist.*

Maltman, A. (1984). On the term "soft-sediment deformation." *Journal of Structural Geology, 6*(5), 589–592. https://doi.org/10.1016/0191-8141(84)90069-5

Maltman, A. J. (Ed.). (1994). *The geological deformation of sediments*. Springer.

Martín-Chivelet, J., Palma, R. M., López-Gómez, J., & Kietzmann, D. A. (2011). Earthquake-induced soft-sediment deformation structures in Upper Jurassic open-marine microbialites (Neuquén Basin, Argentina). *Sedimentary Geology, 235*(3–4), 210–221. https://doi.org/10.1016/j.sedgeo.2010.09.017

Martín-Martín, J. D., Vergés, J., Saura, E., Moragas, M., Messager, G., Baqués, V., Razin, P., Grélaud, C., Malaval, M., Joussiaume, R., Casciello, E., Cruz-Orosa, I., & Hunt, D. W. (2017). Diapiric growth within an Early Jurassic rift basin: The Tazoult salt wall (central High Atlas, Morocco). *Tectonics, 36*(1), 2–32. https://doi.org/10.1002/2016TC004300

Marzoli, A., Bertrand, H., Youbi, N., Callegaro, S., Merle, R., Reisberg, L., Chiaradia, M., Brownlee, S., Jourdan, F., Zanetti, A., Davies, J., Cuppone, T., Mahmoudi, A., Medina, F., Renne, P. R., Bellieni, G., Crivellari, S., El Hachimi, H., Bensalah, M. K., … Tegner, C. (2019). The Central Atlantic Magmatic Province (CAMP) in Morocco. *Journal of Petrology, 60*(5), 945–996. https://doi.org/10.1093/petrology/egz021

Marzoli, A., Renne, P. R., Piccirillo, E. M., Ernesto, M., Bellieni, G., & Min, A. D. (1999). Extensive 200-million-year-old continental flood basalts of the Central Atlantic Magmatic Province. *Science, 284*(5414), 616–618. https://doi.org/10.1126/science.284.5414.616

Masrour, M., Boutakiout, M., Gascón, J. H., De Zuazo, J. L. S. R., Martínez, R. O., & Pérez-Lorente, F. (2020). Footprints of Batrachopus isp. From the Imilchil megatracksite. Middle? -Upper Jurassic, central High Atlas (Morocco). *Journal of African Earth Sciences, 172*, 103980. https://doi.org/10.1016/j.jafrearsci.2020.103980

Mattauer, M., Tapponnier, P., & Proust, F. (1977). Sur les mecanismes de formation des chaines intracontinentales; l'exemple des chaines atlasiques du Maroc. *Bulletin De La Société Géologique De France, 7*(3), 521–526. https://doi.org/10.2113/gssgfbull.S7-XIX.3.521

Medina, F., & Cherkaoui, T. E. (2021). The Midelt earthquake of November 17th 2019, and its implications on the present-day tectonics of the junction of the High and Middle Atlas (Morocco). *Arabian Journal of Geosciences, 14*(17), 1–18. https://doi.org/10.1007/s12517-021-07853-2

Miall, A. D. (1978). Lithofacies types and vertical profile models in braided rivers deposits: A summary. In A. D. Miall (Ed.), *Fluvial Sedimentology* (pp. 597–604). Memoir, 5. *Canadian Society of Petroleum Geologists*, Calgary.

Miall, A. D. (2006). *The Geology of Fluvial Deposits: Sedimentary facies, basin analysis and petroleum geology*. Springer Verlag.

Michard, A., Ibouh, H., & Charrière, A. (2011). Syncline-topped anticlinal ridges from the High Atlas: A Moroccan conundrum, and inspiring structures from the Syrian Arc, Israel. *Terra Nova, 23*(5), 314–323. https://doi.org/10.1111/j.1365-3121.2011.01016.x

Midwinter, D., Hadlari, T., & Dewing, K. (2017). Lower Triassic river-dominated deltaic successions from the Sverdrup Basin, Canadian Arctic. *Palaeogeography, Palaeoclimatology, Palaeoecology, 476*, 55–67. https://doi.org/10.1016/j.palaeo.2017.03.017

Miller, M. S., & Becker, T. W. (2014). Reactivated lithospheric-scale discontinuities localize dynamic uplift of the Moroccan Atlas Mountains. *Geology, 42*(1), 35–38. https://doi.org/10.1130/G34959.1

Montenat, C., Barrier, P., & Hibsch, C. (2007). Seismites: An attempt at critical analysis and classification. *Sedimentary Geology, 196*(1–4), 5–30. https://doi.org/10.1016/j.sedgeo.2006.08.004

Moragas, M. (2017). Multidisciplinairy Characterization of Diapiric Basins Integrating Field Examples, Numerical and Analogue Modelling: Central High Atlas Basin (Morocco). *Ph.D thesis*. University of Barcelona, Barcelona.

Moragas, M., Vergés, J., Saura, E., Martín-Martín, J. D., Messager, G., Merino-Tomé, Ó., Suárez-Ruiz, I., Razin, P., Grélaud, C., Malaval, M., Joussiaume, R., & Hunt, D. W. (2018). Jurassic rifting to post-rift subsidence analysis in the Central High Atlas and its relation to salt diapirism. *Basin Research, 30*, 336–362. https://doi.org/10.1111/bre.12223

Moretti, M. (2000). Soft-sediment deformation structures interpreted as seismites in middle-late Pleistocene aeolian deposits (Apulian foreland, southern Italy). *Sedimentary Geology, 135*(1–4), 167–179. https://doi.org/10.1016/S0037-0738(00)00070-1

Moretti, M., Alfaro, P., Caselles, O., & Canas, J. A. (1999). Modelling seismites with a digital shaking table. *Tectonophysics, 304*(4), 369–383. https://doi.org/10.1016/S0040-1951(98)00289-3

Moretti, M., & Sabato, L. (2007). Recognition of trigger mechanisms for soft-sediment deformation in the Pleistocene lacustrine deposits of the Sant'Arcangelo Basin (Southern Italy): seismic shock vs. overloading. *Sedimentary Geology, 196*(1–4), 31–45. https://doi.org/10.1016/j.sedgeo.2006.05.012

Moretti, M., & van Loon, A. T. (2014). Restrictions to the application of 'diagnostic' criteria for recognizing ancient seismites. *Journal of Palaeogeography, 3*(2), 162–173. https://doi.org/10.3724/SP.J.1261.2014.00050

Morsilli, M., Bucci, M. G., Gliozzi, E., Lisco, S., & Moretti, M. (2020). Sedimentary features influencing the occurrence and spatial variability of seismites (late Messinian, Gargano Promontory, southern Italy). *Sedimentary Geology, 401*, 105628. https://doi.org/10.1016/j.sedgeo.2020.105628

Neuwerth, R., Suter, F., Guzman, C. A., & Gorin, G. E. (2006). Soft-sediment deformation in a tectonically active area: The Plio-Pleistocene Zarzal Formation in the Cauca Valley (Western Colombia). *Sedimentary Geology, 186*(1–2), 67–88. https://doi.org/10.1016/j.sedgeo.2005.10.009

Nichols, G. J., & Fisher, J. A. (2007). Processes, facies and architecture of fluvial distributary system deposits. *Sedimentary Geology, 195*(1–2), 75–90. https://doi.org/10.1016/j.sedgeo.2006.07.004

Nichols, R. J. (1995). The liquification and remobilization of sandy sediments. *Geological Society, London, Special Publication, 94*, 63–76. https://doi.org/10.1144/GSL.SP.1995.094.01.06

Nichols, R. J., Sparks, R. S. J., & Wilson, C. J. N. (1994). Experimental studies of the fluidization of layered sediments and the formation of fluid escape structures. *Sedimentology, 41*(2), 233–253. https://doi.org/10.1111/j.1365-3091.1994.tb01403.x

Ninfo, A., Zizioli, D., Meisina, C., Castaldini, D., Zucca, F., Luzi, L., & De Amicis, M. (2012). The survey and mapping of sand-boil landforms related to the Emilia 2012 earthquakes: preliminary results. *Annals of Geophysics*. https://doi.org/10.4401/ag-6114

Noffke, N., Beraldi-Campesi, H., Callefo, F., Carmona, N. B., Cuadrado, D. G., Hickman-Lewis, K., Homann, M., Mitchell, R., Sheldon, N., Westall, F. & Xiao, S. (2022). Part B, Volume 2, Chapter 5: *Microbially induced sedimentary structures (MISS)* (pp. 1–29). *Treatise Online*, 162.

Noffke, N., Gerdes, G., Klenke, T., & Krumbein, W. E. (2001). Microbially induced sedimentary structures: A new category within the classification of primary sedimentary structures. *Journal of Sedimentary Research, 71*(5), 649–656. https://doi.org/10.1306/2DC4095D-0E47-11D7-8643000102C1865D

Obermeier, S.F., Pond, E.C., Olson, S.M., & Green, R.A. (2002). Paleoliquefaction studies in continental settings. In F.R. Ettensohn, N. Rast, & C.E. Brett (Eds.), *Ancient seismites* (pp. 13–27). *Geological Society of America Special Paper 359*. https://doi.org/10.1130/0-8137-2359-0.13

Obermeier, S.F. (2009). Using liquefaction-induced and other soft-sediment features for paleoseismic analysis. In M. Calpin (Ed.), *Paleoseismology: International Geophysics Series* (2nd ed., pp. 497–564). Elsevier. https://doi.org/10.1016/S0074-6142(09)95007-0

Obermeier, S. F. (1996). Use of liquefaction-induced features for paleoseismic analysis—an overview of how seismic liquefaction features can be distinguished from other features and how their regional distribution and properties of source sediment can be used to infer the location and strength of Holocene paleoearthquakes. *Engineering Geology, 44*(1–4), 1–76. https://doi.org/10.1016/S0013-7952(96)00040-3

Onasch, C.M., & Kahle, C.F. (2002). Seismically induced soft-sediment deformation in some Silurian carbonates, eastern U.S. Midcontinent. In F.R. Ettensohn, N. Rast, & C.E. Brett (Eds.), *Ancient Seismites* (pp. 165–176). *Geological Society of America Special Paper 359*. https://doi.org/10.1130/0-8137-2359-0.165

Ouabid, M., Raji, O., Dautria, J. M., Bodinier, J. L., Parat, F., El Messbahi, H., Garrido, C. J., & Ahechach, Y. (2021). Petrological and geochemical constraints on the origin of apatite ores from Mesozoic alkaline intrusive complexes, Central High-Atlas, Morocco. *Ore Geology Reviews, 136*, 104250. https://doi.org/10.1016/j.oregeorev.2021.104250

Ouaskou, M., Charrière, A., Boumir, K., Ouarhache, D., Ferrière, J., Ibouh, H., Feist, M., Oussou, A., Lakbir, M., Ech-charray, K., & Haddoumi, H. (2021). Barremian intracontinental rift and Aptian Atlantic transgression in the northern boundary of the Central High Atlas (Morocco). *Journal of African Earth Sciences, 175*, 104094. https://doi.org/10.1016/j.jafrearsci.2020.104094

Oukassou, M., Klein, H., Lagnaoui, A., Charrière, A., Saber, H., Gierliński, G. D., Lallensack, J. N., Hminna, A., Boumaalif, A., Oussou, A., & Ouarhache, D. (2019). Polyonyx-like tracks from Middle-? Upper Jurassic red beds of Morocco: Implications for sauropod communities on southern margins of tethys. *Palaeogeography, Palaeoclimatology, Palaeoecology, 536*, 109394. https://doi.org/10.1016/j.palaeo.2019.109394

Oussou, A., Falkingham, P. L., Butler, R. J., Boumir, K., Ouarhache, D., Ech-charay, K., Charrière, A., & Maidment, S. C. R. (2023). New Middle to? Late Jurassic dinosaur tracksites in the Central High Atlas Mountains. *Morocco. Royal Society Open Science, 10*, 231091. https://doi.org/10.1098/rsos.231091

Owen, G., Moretti, M., & Alfaro, P., (Eds.). (2011a). Recognising triggers for soft-sediment deformation: Current understanding and future directions [Special issue]. *Sedimentary Geology 235*.

Owen, A., Nichols, G. J., Hartley, A. J., Weissmann, G. S., & Scuderi, L. A. (2015). Quantification of a distributive fluvial system: The Salt Wash DFS of the Morrison Formation, SW USA. *Journal of Sedimentary Research, 85*(5), 544–561. https://doi.org/10.2110/jsr.2015.35

Owen, G. (1987). Deformation processes in unconsolidated sands. *Geological Society of London Special Publication, 29*, 11–24. https://doi.org/10.1144/GSL.SP.1987.029.01.02

Owen, G. (1996). Experimental soft-sediment deformation: Structures formed by the liquefaction of unconsolidated sands and some ancient examples. *Sedimentology, 43*(2), 279–293. https://doi.org/10.1046/j.1365-3091.1996.d01-5.x

Owen, G. (2003). Load structures: Gravity-driven sediment mobilization in the shallow subsurface. *Geological Society of London Special Publication, 216*, 21–34. https://doi.org/10.1144/GSL.SP.2003.216.01.03

Owen, G., & Moretti, M. (2011). Identifying triggers for liquefaction-induced soft-sediment deformation in sands. *Sedimentary Geology, 235*(3–4), 141–147. https://doi.org/10.1016/j.sedgeo.2010.10.003

Owen, G., Moretti, M., & Alfaro, P. (2011b). Recognising triggers for soft-sediment deformation: current understanding and future directions. *Sedimentary Geology, 235*(3–4), 133–140. https://doi.org/10.1016/j.sedgeo.2010.12.010

Ozcelik, M. (2016). Evaluation of soft sediment deformation structures along the Fethiye-Burdur Fault Zone, SW Turkey. *Journal of Earth System Science, 125*(2), 343–358. https://doi.org/10.1007/s12040-016-0671-4

Panfili, G., Cirilli, S., Dal Corso, J., Bertrand, H., Medina, F., Youbi, N., & Marzoli, A. (2019). New biostratigraphic constraints show rapid emplacement of the Central Atlantic Magmatic Province (CAMP) during the end-Triassic mass extinction interval. *Global and Planetary Change, 172*, 60–68. https://doi.org/10.1016/j.gloplacha.2018.09.009

Pillai, S. P., & Kale, V. S. (2011). Seismites in the Lokapur Subgroup of the Proterozoic Kaladgi Basin, South India: A testimony to syn-sedimentary tectonism. *Sedimentary Geology, 240*(1–2), 1–13. https://doi.org/10.1016/j.sedgeo.2011.06.013

Plaziat, J. C., Aberkan, M. H., & Reyss, J. L. (2006). New late Pleistocene seismites in a shoreline series including eolianites, north of Rabat (Morocco). *Bulletin De La Société Géologique De France, 177*(6), 323–332. https://doi.org/10.2113/gssgfbull.177.6.323

Plaziat, J. C., & Ahamamou, M. (1998). Les différents mécanismes à l'origine de la diversité des séismites, leur identification dans le Pliocène du Saïss de Fès et de Meknès (Maroc) et leur signification tectonique. *Geodinamica Acta, 11*(4), 183–203. https://doi.org/10.1016/S0985-3111(98)80004-1

Plink-Björklund, P. (2021). Distributive Fluvial Systems: Fluvial and Alluvial Fans. In A. Alderton & S.A. Elias (Eds.), *Encyclopedia of Geology* (2nd Ed., Vol. 2, pp. 745–758). Academic Press, UK.

Rodríguez-Pascua, M. A., Calvo, J. P., De Vicente, G., & Gómez-Gras, D. (2000). Soft-sediment deformation structures interpreted as seismites in lacustrine sediments of the Prebetic Zone, SE Spain, and their potential use as indicators of earthquake magnitudes during the Late Miocene. *Sedimentary Geology, 135*(1–4), 117–135. https://doi.org/10.1016/S0037-0738(00)00067-1

Rowan, M. G., Muñoz, J. A., Giles, K. A., Roca, E., Hearon, T. E., IV., Fiduk, J. C., Ferrer, O., & Fischer, M. P. (2020). Folding and fracturing of rocks adjacent to salt diapirs. *Journal of Structural Geology, 141*, 104187. https://doi.org/10.1016/j.jsg.2020.104187

Rudersdorf, A., Hartmann, K., Yu, K., Stauch, G., & Reicherter, K. (2015). Seismites as indicators for Holocene seismicity in the northeastern Ejina Basin, Inner Mongolia. *Geological Society, London, Special Publications, 432*(1), 213–231. https://doi.org/10.1144/SP432.6

Saura, E., Vergés, J., Martín-Martín, J. D., Messager, G., Moragas, M., Razin, P., Grélaud, C., Joussiaume, R., Malaval, M., Homke, S., & Hunt, D. W. (2014). Syn-to post-rift diapirism and minibasins of the Central High Atlas (Morocco): The changing face of a mountain belt. *Journal of the Geological Society, 171*(1), 97–105. https://doi.org/10.1144/jgs2013-079

Seilacher, A. (1969). Fault-graded beds interpreted as seismites. *Sedimentology, 13*(1–2), 155–159. https://doi.org/10.1111/j.1365-3091.1969.tb01125.x

Shiki, T., Cita, M.B., & Gorsline, D.S. (Eds.). (2000). Sedimentary Features of Seismites, Seismo-Turbidites and Tsunamiites [Special issue]. *Sedimentary Geology 135*. https://doi.org/10.1016/S0037-0738(00)00058-0

Sims, J.D. (2013). Earthquake-induced load casts, pseudonodules, ball-and-pillow structures, and convolute lamination: Additional deformation structures for paleoseismic studies. In R.T. Cox, M.P. Tuttle, O.S. Boyd, J. Locat (Eds.), *Recent Advances in North American Paleoseismology and Neotectonics East of the Rockies* (pp. 191–201). Geological Society of America, Special Paper, 493. https://doi.org/10.1130/2012.2493(09)

Sims, J. D. (1975). Determining earthquake recurrence intervals from deformational structures in young lacustrine sediments.

Tectonophysics, 29, 141–152. https://doi.org/10.1016/0040-1951(75)90139-0

Slingerland, R., & Smith, N. D. (2004). River avulsions and their deposits. *Annual Review of Earth and Planetary Sciences, 32*, 257–285. https://doi.org/10.1146/annurev.earth.32.101802.120201

Smith, G.J., & Jacobi, R.D. (2002). Anomalous paleoflow orientations: A potential methodology for determining recurrence rates and magnitudes in paleoseismic studies of syndepositional faults. In F.R. Ettensohn, N. Rast, & C.E. Brett (Eds.), *Ancient Seismites* (pp. 145–164). Geological Society of America Special Paper 359. https://doi.org/10.1130/0-8137-2359-0.145

Spalluto, L., Moretti, M., Festa, V., & Tropeano, M. (2007). Seismically-induced slumps in Lower-Maastrichtian peritidal carbonates of the Apulian Platform (southern Italy). *Sedimentary Geology, 196*(1–4), 81–98. https://doi.org/10.1016/j.sedgeo.2006.06.009

Storti, F., & Vannucchi, P. (Eds.). (2007). Deformation of Soft Sediment in Nature and Laboratory [Special issue]. *Sedimentary Geology 196*(1–4).

Studer, M.R. (1987). Tectonique et Pétrographie des roches sédimentaires, éruptives et métamorphiques de la région de Tounfite-Tirrhist. (Haut Atlas central, Mésozoïque, Maroc). *Notes et Mémoires du Service Géologique du Maroc, 43*(321), 65–197.

Suter, F., Martínez, J. I., & Vélez, M. I. (2011). Holocene soft-sediment deformation of the Santa Fe–Sopetrán Basin, northern Colombian Andes: Evidence for pre-Hispanic seismic activity? *Sedimentary Geology, 235*(3–4), 188–199. https://doi.org/10.1016/j.sedgeo.2010.09.018

Taşgın, C. K., Orhan, H., Türkmen, İ, & Aksoy, E. (2011). Soft-sediment deformation structures in the late Miocene Şelmo Formation around Adıyaman area, Southeastern Turkey. *Sedimentary Geology, 235*(3–4), 277–291. https://doi.org/10.1016/j.sedgeo.2010.08.005

Teixell, A., Arboleya, M. L., Julivert, M., & Charroud, M. (2003). Tectonic shortening and topography in the central High Atlas (Morocco). *Tectonics*. https://doi.org/10.1029/2002TC001460

Teixell, A., Ayarza, P., & Arboleya, M. L. (2014). Reactivated lithospheric-scale discontinuities localize dynamic uplift of the Moroccan Atlas Mountains: COMMENT. *Geology, 42*(5), e336–e336. https://doi.org/10.1130/G35510C.1

Teixell, A., Barnolas, A., Rosales, I., & Arboleya, M. L. (2017). Structural and facies architecture of a diapir-related carbonate minibasin (lower and middle Jurassic, High Atlas, Morocco). *Marine and Petroleum Geology, 81*, 334–360. https://doi.org/10.1016/j.marpetgeo.2017.01.003

Törő, B., & Pratt, B. R. (2016). Sedimentary record of seismic events in the Eocene Green River Formation and its implications for regional tectonics on lake evolution (Bridger Basin, Wyoming). *Sedimentary Geology, 344*, 175–204. https://doi.org/10.1016/j.sedgeo.2016.02.003

Torres-López, S., Casas, A. M., Villalaín, J. J., El Ouardi, H., & Moussaid, B. (2016). Pre-Cenomanian vs. Cenozoic folding in the High Atlas revealed by palaeomagnetic data. *Terra Nova, 28*(2), 110–119. https://doi.org/10.1111/ter.12197

van Loon, A. J. (1992). The recognition of soft-sediment deformations as early-diagenetic features: A literature review. In K. H. Wolf & G. V. Chilingarian (Eds.), *Diagenesis III: Developments in Sedimentology* (pp. 135–189). Elsevier. https://doi.org/10.1016/S0070-4571(08)70565-X

Van Rensbergen, P., Hillis, R.R., Maltman, A.J., Morley, C.K. (Eds.). (2003). Subsurface Sediment Mobilization. *Geological Society, London, Special Publications, 216*. https://doi.org/10.1144/GSL.SP.2003.216

van Loon, A. J. (2009). Soft-sediment deformation structures in siliciclastic sediments: an overview. *Geologos*, *15*.

van Loon, A.J., (Ed.). (2014a). Seismites and their soft-sediment deformation structures [Special issue]. *Geologos 20 (2),* 61–166.

van Loon, A. T. (2014). The life cycle of seismite research. *Geologos, 20*(2), 61–66. https://doi.org/10.2478/logos-2014-0005

van Loon, A. J., & Wiggers, A. J. (1976). Metasedimentary "graben" and associated structures in the lagoonal Almere Member (Groningen Formation, The Netherlands). *Sedimentary Geology, 16*(4), 237–254. https://doi.org/10.1016/0037-0738(76)90001-4

Vergés, J., Moragas, M., Martín-Martín, J. D., Saura, E., Casciello, E., Razin, Ph., Grelaud, C., Malaval, M., Joussiaume, R., Messager, G., Sharp, I., & Hunt, D. W. (2017). Salt tectonics in the Atlas Mountains of Morocco. In J. I. Soto, J. F. Flinch, & G. Tari (Eds.), *Permo-Triassic Salt Provinces of Europe, North Africa and the Atlantic Margins* (pp. 563–579). Elsevier. https://doi.org/10.1016/B978-0-12-809417-4.00027-6

Waldron, J. W., & Gagnon, J. F. (2011). Recognizing soft-sediment structures in deformed rocks of orogens. *Journal of Structural Geology, 33*(3), 271–279. https://doi.org/10.1016/j.jsg.2010.06.015

Warme, J. E. (1988). Jurassic carbonate facies of the central and eastern high Atlas rift, Morocco. In V. Jacobshagen (Ed.), *The Atlas System of Morocco* (pp. 169–199). Springer Verlag. https://doi.org/10.1007/BFb0011593

Weissmann, G. S., Hartley, A. J., Ab, A., Scuderi, L. A., Nichols, G. J., Davidson, S. K., Owen, A., Atchley, S. C., Bhattacharyya, P., Michel, L., & Tabor, N. J. (2013). Prograding distributive fluvial systems-geomorphic models and ancient examples. In S. G. Driese, L. C. Nordt, & P. J. McCarthy (Eds.), *New Frontiers in Paleopedology and Terrestrial Paleoclimatology* (pp. 131–147). SEPM Special Publication 104. https://doi.org/10.2110/sepmsp.104

Wheeler, R.L. (2002). Distinguishing seismic from nonseismic soft-sediment structures: criteria from seismic-hazard analysis. In F.R. Ettensohn, N. Rast, & C.E. Brett (Eds.), *Ancient Seismites* (pp. 1–11). Geological Society of America Special Paper 359. https://doi.org/10.1130/0-8137-2359-0.1

Yang, R., & van Loon, A. T. (2016). Early Cretaceous slumps and turbidites with peculiar soft-sediment deformation structures on Lingshan Island (Qingdao, China) indicating a tensional tectonic regime. *Journal of Asian Earth Sciences, 129*, 206–219. https://doi.org/10.1016/j.jseaes.2016.08.014

Zanchi, A. (1992). Tectonic and liquefaction structures in the Loreto basin, Baja California (Mexico): Synsedimentary deformation along a fossil fault plane. *Geodinamica Acta, 5*(3), 187–201. https://doi.org/10.1080/09853111.1992.11105227

Zarki, H., Macaire, J. J., Beck, C., & De Luca, P. (2004). Morpho-sedimentary evolution of the lower Moulouya (North Eastern Morocco) during middle and upper Holocene. *Seismicity and Neotectonic Effects. Geodinamica Acta, 17*(3), 205–217. https://doi.org/10.3166/ga.17.205-217

Zayane, R., Essaifi, A., Maury, R. C., Piqué, A., Laville, E., & Bouabdelli, M. (2002). Cristallisation fractionnée et contamination crustale dans la série magmatique jurassique transitionnelle du Haut Atlas central (Maroc). *Comptes Rendus Geoscience, 334*(2), 97–104. https://doi.org/10.1016/S1631-0713(02)01716-9

Zeng, M., Ettensohn, F. R., & Spangenberg, J. E. (2018). Bedding-parallel lenticular soft-sediment deformation structures: A type of seismite in extensional settings. *Tectonophysics 747*, 128–145. https://doi.org/10.1016/j.tecto.2018.10.001